

---

# A Single Merging Suffices: Recovering Server-based Learning Performance in Decentralized Learning

---

Tongtian Zhu<sup>1\*</sup>, Tianyu Zhang<sup>2,3\*</sup>, Mingze Wang<sup>4</sup>, Zhanpeng Zhou<sup>5†</sup>, Can Wang<sup>1</sup>

1 Zhejiang University 2 Mila - Quebec AI Institute 3 Université de Montréal

4 Peking University 5 Shanghai Jiao Tong University

{raidan, wchang}@zju.edu.cn

tianyu.zhang@mila.quebec mingzewang@stu.pku.edu.cn zzp1012@sjtu.edu.cn

## Abstract

Decentralized learning provides a scalable alternative to traditional parameter-server-based training, yet its performance is often hindered by limited peer-to-peer communication. In this paper, we study how communication should be scheduled over time, including determining when and how frequently devices synchronize. Our empirical results show that concentrating communication budgets in the later stages of decentralized training markedly improves global generalization. Surprisingly, we uncover that fully connected communication at the final step, implemented by a single global merging, is sufficient to match the performance of server-based training. We further show that low communication in decentralized learning preserves the *mergeability* of local models throughout training. Our theoretical contributions, which explain these phenomena, are first to establish that the globally merged model of decentralized SGD can converge faster than centralized mini-batch SGD. Technically, we novelly reinterpret part of the discrepancy among local models, which were previously considered as detrimental noise, as constructive components that accelerate convergence. This work challenges the common belief that decentralized learning generalizes poorly under data heterogeneity and limited communication, while offering new insights into model merging and neural network loss landscapes. The code will be made publicly available soon.

## 1 Introduction

Decentralized learning offers a promising approach to crowdsource computational workloads across geographically distributed compute [100, 6, 39]. A defining characteristic of this setting is the reliance on peer-to-peer communication during training, involving the peer-level exchange of model parameters or gradients during training. However, such communication is often constrained in practice due to limited bandwidth between geographically distant nodes, making it a scarce resource.

These constraints can significantly degrade the performance of decentralized learning, both theoretically and empirically [53, 42, 86]. As a result, efficiently allocating limited communication resources becomes a fundamental challenge in decentralized learning, especially in heterogeneous environments where local data distributions vary across nodes [58].

To date, most efforts addressing this challenge have focused on optimizing communication allocation at the *spatial level*, particularly through the design of communication graphs [99, 51, 82, 40]. In contrast, few works have attempted to study how communication should be allocated over temporal levels, i.e., when and how frequently agents synchronize parameters or gradients with others. Ex-

---

\*Equal contribution. † Corresponding author.

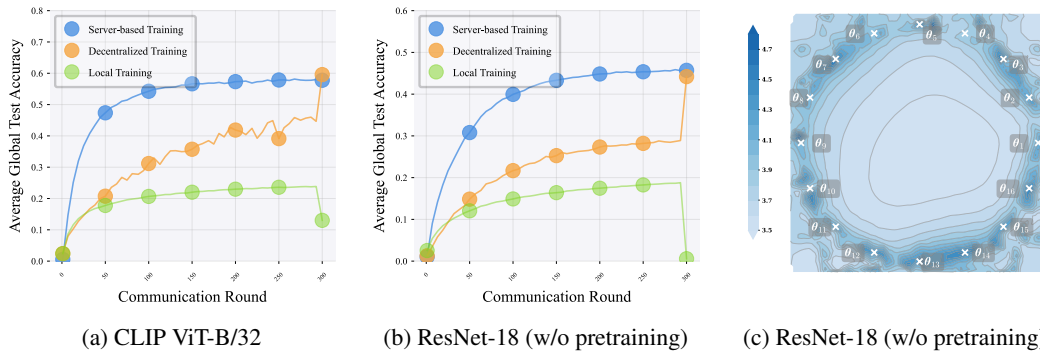


Figure 1: **(a, b)**: Comparisons of global test accuracy (see Definition 2) in training of CLIP ViT-B/32 (a) and ResNet-18 (b) on the Tiny ImageNet dataset, distributed across 16 agents with high heterogeneity (Dirichlet  $\alpha = 0.1$ ; see details in Appendix C.1). Decentralized training here involves each agent syncing with a random peer per round. A single global model merging is performed at the final round. **(c)**: Loss landscape of decentralized training (w/o permutation) before global merging, under the same setup as the orange curve in (b);  $\{\theta_k\}_{k=1}^{16}$  denotes the local models.

ploring the communication allocation problem at the temporal levels is of significant importance to improve the efficiency and generalization of decentralized learning.

**Question:** *How to allocate communication budget in decentralized learning over temporal levels?*

To answer this question, we design a series of experiments that allocate communication budgets across different time windows during training (see Figure 3). Specifically, we divide the training process into consecutive windows, each consisting of a fixed number of communication rounds. We assign higher communication budgets to selected windows using global synchronization via AllReduce [76], while keeping communication low otherwise by infrequent synchronization with random peer agents.<sup>2</sup> This setup enables us to systematically examine how the temporal communication allocations influence final global performance under constrained budgets. We observe that allocating higher communication budgets toward the later stages of training consistently leads to improved final global test performance. More surprisingly, we find that even a single round of fully-connected communication<sup>3</sup> at the final step, implemented as a global merging, can recover the server-based training<sup>4</sup> performance (see Figure 1a and Figure 1b). See Figure 2 for a comparative illustration of different training schemes.

**Surprising Phenomenon:** *A single global merging of decentralized models, even under severely constrained communication and high data heterogeneity, can recover server-based training performance.*

Further results show that, throughout training, the average of local models in decentralized learning consistently achieves higher global test accuracy than individual models (see Figure 1c and Figure 3c), a property we refer to as *mergeability* (see Definition 1). While extensive studies suggest that merging independently trained models typically leads to an increased loss [21, 1], we show that local models in decentralized learning remain mergeable and can approach and even surpass the performance of server-based training after merging. Our findings challenge the conventional belief that decentralized learning fails to generalize under high data heterogeneity and limited communication, and offer new insights into model merging techniques [91, 72] and loss landscape of neural networks [21, 18].

Subsequently, we delve deeper into the mechanism behind the *mergeability* of local models in decentralized learning. We make an initial attempt by analyzing the convergence of decentralized SGD (DSGD) in a finer-grained manner. We theoretically establish that the globally merged model of

<sup>2</sup>Agents here refer to participants or nodes in the decentralized learning system.

<sup>3</sup>Fully-connected communication refers to global synchronization via AllReduce. In this paper, fully-connected communication is realized through parameter averaging over the models on all agents, namely *global merging*.

<sup>4</sup>"Server-based training" refers to training schemes coordinated by central servers, e.g., federated learning. See Figure 2 for a comparative illustration of different training schemes.

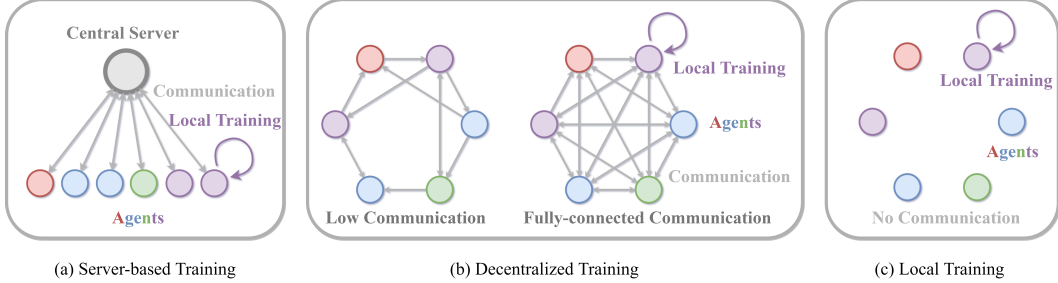


Figure 2: A comparative illustration of server-based, decentralized, and local training.

DSGD can achieve faster convergence than centralized mini-batch SGD [15, 49].<sup>5</sup> Our key technical novelty lies in a novel treatment of consensus violation, which characterizes the discrepancy among local models. In contrast to prior work that considers such violations as purely detrimental noise, we partially incorporate them as constructive components to accelerate convergence.

**Our Contributions.** In summary, our work focuses on the temporal communication allocation in decentralized learning, which has not been carefully studied yet. We show that a single global merging at the end of training is sufficient for decentralized learning to match the global generalization performance of server-based learning. We summarize our main contributions as follows.

- **Empirical Observations. (1):** We highlight the critical role of allocating communication towards the later stages of decentralized training. Remarkably, a single global merging at the final step can recover server-based training performance, even under severe communication constraints and data heterogeneity (see Figure 1a, Figure 1b and additional results in Appendix C.2). **(2):** Low communication throughout training preserves the mergeability of local models throughout training (blue curve in Figure 3c), which does not hold under fully local training (orange curve in Figure 3c).
- **Theoretical Contributions.** We provide the first convergence analysis showing that the globally merged model of decentralized SGD can outperform centralized mini-batch SGD (Theorem 1 and Proposition 2), by partially incorporating consensus violations as constructive components to accelerate convergence. Furthermore, we offer a theoretical explanation for why communication should be concentrated in the later stages of decentralized training, and why limited but nonzero communication can ensure mergeability (see Proposition 3).

We provide additional insights and address potential concerns in a Q&A Section (see Appendix A).

## 2 Related Work

**Temporal Communication Allocation in Decentralized Learning.** Despite extensive work focusing on communication allocation at the spatial level in decentralized learning (e.g., design communication topology) [99, 51, 82, 40], few studies have examined the communication allocation problem over temporal levels. In the server-based setting, Gu et al. [28] proposed a strategy for scheduling the number of local steps based on insights into the implicit bias of local SGD [29]. In decentralized learning, Kong et al. [43] demonstrated that in IID scenarios, aligning local models more closely with their global average through high communication early in training modestly improves generalization. Their findings are not at odds with our suggestion to prioritize communication budgets in the later stages of training, as in IID cases, the global population risk  $\mathcal{L}(\cdot)$  reduces to the local population risk  $\mathcal{L}_k(\cdot)$  (see Equation (1)). Therefore, their results primarily address local generalization, as opposed to the global generalization targeted in our work. Another related study by Yuan et al. [100] partitioned language models into computational tasks and scheduled them across heterogeneous devices. While their work developed algorithms for allocating computation, it did not explicitly consider the problem of communication allocation. The research gap in the existing literature motivates our focus on designing temporal communication strategies for decentralized learning.

**Mode Connectivity and Model Merging Techniques.** Recent works on (*Linear*) *Mode Connectivity* have advanced our understanding of the complex loss landscape in neural networks. Freeman

<sup>5</sup>“Centralized mini-batch SGD” refers to parallel SGD training, with synchronization realized by a central server.

and Bruna [22], Draxler et al. [17], Garipov et al. [26], Nagarajan and Kolter [63], Frankle et al. [21] discovered that different solutions of deep neural networks can be merged together by simply averaging their parameters. Sonthalia et al. [80] further showed that the solutions may form a star domain. We note that these phenomenon are observed in the following scenarios:

- *Shared initialization* [21, 20, 107]. Models are initialized from a pretrained checkpoint.
- *Homogeneous data distribution* [91]. Models are trained on homogeneous data distribution.
- *Permutation* [1, 18]. Models are independently trained. The neurons of one model are permuted to match the neurons of the other while maintaining a functionally equivalent network.

These findings have inspired a range of model merging techniques for various applications. Izmailov et al. [38], Matena and Raffel [59], Rame et al. [72, 71], Wortsman et al. [91, 92] found that merging the parameters of models that start from the same pretrained model and finetune over the same task leads to improved generalization and robustness. Furthermore, Ilharco et al. [37], Li et al. [50], Ilharco et al. [36], Ortiz-Jimenez et al. [67], Yadav et al. [96] showed that merging models that finetune over different tasks enables multi-task abilities.

In contrast, our results show that mode connectivity, or mergeability, can still emerge in decentralized learning, even when the local models are initialized *differently*, trained on highly *heterogeneous* data, and merged *without* any permutation. Our findings offer new insights into both model merging techniques and the geometry of the neural network loss landscape, which we anticipate will motivate further advances in both areas.

### 3 Notations and Preliminaries

#### 3.1 Decentralized Learning

Decentralized learning formalizes distributed training as an optimization problem over a connected graph  $G = (\mathcal{V}, \mathcal{E})$ , where  $\mathcal{V}$  is the set of  $m$  agents and  $\mathcal{E}$  denotes the communication links. Each agent  $k \in \mathcal{V}$  samples data from a local distribution  $\mathcal{D}_k$  and maintains a local model  $\theta_k \in \mathbb{R}^d$ . The objective is to learn a consensus model  $\theta$  that minimizes the global population risk [42, 19]:

$$\min_{\theta \in \mathbb{R}^d} \left[ \mathcal{L}(\theta) \triangleq \frac{1}{m} \sum_{k \in \mathcal{V}} \mathbb{E}_{\xi_k \sim \mathcal{D}_k} \mathcal{L}(\theta; \xi_k) \right], \quad (1)$$

where  $\mathbb{E}_{\xi_k \sim \mathcal{D}_k} \mathcal{L}(\theta; \xi_k) \triangleq \mathcal{L}_k(\theta)$  denotes the local population risk of  $\theta$  on unseen instance  $\xi_k \sim \mathcal{D}_k$ .

In practice, the optimization of Equation (1) is performed under the empirical risk minimization framework, leveraging  $m$  local datasets  $S \triangleq \bigcup_{k=1}^m S_k$ , where  $S_k = \{\xi_{k,1}, \dots, \xi_{k,\zeta}\}$  denotes the dataset of agent  $k$  sampled from  $\mathcal{D}_k$ . The resulting optimization problem is given by:

$$\min_{\theta \in \mathbb{R}^d} \left[ \mathcal{L}_S(\theta) \triangleq \frac{1}{m} \sum_{k \in \mathcal{V}} \sum_{\zeta=1}^{n_k} \mathcal{L}(\theta; \xi_{k,\zeta}) \right]. \quad (2)$$

To solve the optimization problem in Equation (2), decentralized algorithms minimize the global empirical risk with only local computations and peer-to-peer communications among agents [84, 65]. The communication graph is governed by a weighted adjacency matrix  $W^{(t)} \in [0, 1]^{m \times m}$ , sampled from a distribution  $\mathcal{W}^{(t)}$ , where each entry  $W_{k,l}^{(t)} \geq 0$  reflects the influence of agent  $l$  on agent  $k$ . Decentralized learning algorithms operate by alternating between local updates and the aggregation of model parameters through communication with neighbors, as outlined in Algorithm 1.

#### 3.2 Mergeability

**Definition 1** (Mergeability under Global Population Risk). *A set of local models  $\{\theta_k\}_{k \in \mathcal{V}}$  is globally mergeable if there exist combination weights  $\{w_k\}_{k \in \mathcal{V}} \geq 0$  such that:*

$$\mathcal{L} \left( \sum_{k \in \mathcal{V}} w_k \theta_k \right) \leq \sum_{k \in \mathcal{V}} w_k \mathcal{L}(\theta_k), \quad (3)$$

where  $\mathcal{L}(\cdot)$  denotes the global population risk.

---

**Algorithm 1** Decentralized Learning

---

**input** Initialize values  $\theta_k^{(0)} \in \mathbb{R}^d$  on each agent  $k \in \mathcal{V}$ , number of steps  $T$ , mixing matrix  $W$

- 1: **in parallel on all agent**  $k \in \mathcal{V}$ , **for**  $t = 0, \dots, T - 1$  **do**
- 2:   Sample training data  $\xi_k^{(t)}$  from  $\mathcal{D}_k$ ,  $\theta_k^{(t+1)} \leftarrow \text{Optimizer}(\theta_k^{(t)}, \xi_k^{(t)})$  ▷ Local update
- 3:   Send  $\theta_k^{(t)}$  to out-neighbor(s) and receive  $\{\theta_l^{(t)}\}_{l \in \mathcal{N}_{\text{in}}(k)}$  from in-neighbor(s) ▷ Communication
- 4:   Sample mixing matrix  $W^{(t)} \sim \mathcal{W}^{(t)}$ ,  $\theta_k^{(t+1)} \leftarrow \sum_{l \in \mathcal{N}_{\text{in}}(k)} W_{k,l}^{(t)} \theta_l^{(t)}$  ▷ Gossip averaging
- 5: **end parallel for**

---

**Definition 1** formalizes the intuition that a linearly interpolated model can perform no worse than the original local models. We emphasize that such mergeability is inherently non-trivial due to the *non-convexity* of the loss function  $\mathcal{L}$ . In the landscapes of neural networks, linear interpolation between independently trained models without permutation typically leads to increased loss, a phenomenon known as the *loss barrier* [21, 1]. This highlights that mergeability is not generally guaranteed.

## 4 Empirical Observations

**Evaluation Metrics.** In decentralized learning, models are often evaluated in the absence of full consensus due to data heterogeneity and limited training time. In this paper, we adopt the *average global test accuracy*, a proxy of average global population risk, as the primary evaluation metric, which quantifies how well local models generalize to the global data distribution.

**Definition 2** (Average Global Test Accuracy). *The average accuracy of agents  $k \in \mathcal{V}$  is defined as:*

$$\underbrace{\overline{\text{Acc}}(\{\theta_k\}_{k \in \mathcal{V}})}_{\text{Average Accuracy across agents}} = \frac{1}{m} \sum_{k \in \mathcal{V}} \text{Acc}(\theta_k), \quad \text{where } \text{Acc}(\cdot) \triangleq \underbrace{\frac{1}{m} \sum_{l \in \mathcal{V}} \mathbb{E}_{\xi_l \sim \mathcal{D}_l} \text{Acc}(\cdot; \xi_l)}_{\text{Test accuracy on the global distribution}} .$$

### 4.1 Increasing Impact of Communication in the Later Stages of Training

To investigate potential solutions to the temporal communication allocation problem outlined in [Section 1](#), we explore a direct strategy: To concentrate communication in a small subset of communication rounds. To this end, we divide the training process into consecutive windows, each consisting of a fixed length of communication rounds. Specifically, the communication scheme is as follows: (1) fully-connected communication (see [Figure 2](#) (b)) is activated only within specific communication windows (i.e., global synchronization via AllReduce [76]); (2) while in all other rounds, each agent communicates only with *one* random peer (see ‘‘Communication Graph’’ in [Appendix C.1](#)).

As shown in [Figure 3](#), training is divided into 10 (a) and 20 (b) communication windows, respectively. The bars in [Figure 3](#) show both the best global test accuracy achieved during training (lighter-colored bars) and the final test accuracy at the end of training (darker-colored bars). Each bar corresponds to one communication window, where fully connected communication is applied *only* to the rounds within that window, while random peer communication is used in all other rounds. For instance, the inset in [Figure 3a](#) presents the complete test accuracy trajectory when fully-connected communication is applied during rounds 150 to 180. A consistent trend emerges: *allocating communication budgets toward the later stages of training yields substantial improvements, particularly in final test accuracy.*

We further observe a surge-and-decline pattern in performance during high-communication phases (see the insets in [Figure 3a](#) and [Figure 3b](#)). Specifically, transitioning from low to high communication induces a sharp increase in test accuracy. However, this improvement is short-lived, as the performance quickly drops once it returns to low communication. We discuss this phenomenon in [Subsection 4.3](#).

### 4.2 A Single Global Merging Significantly Improves Global Generalization

In [Figure 3b](#), we reduce the fully-connected communication window length to 10 rounds, yet still observe substantial improvements in global generalization. This observation naturally raises the question: *What happens if the fully-connected window is reduced to a single round?*

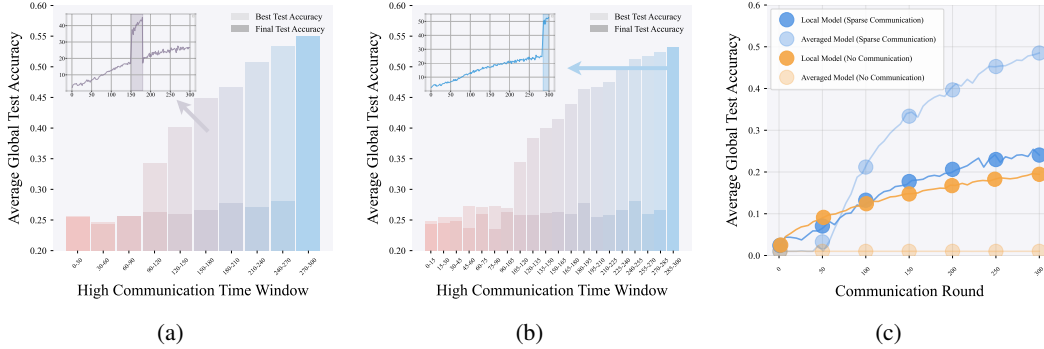


Figure 3: **(a, b)**: Comparisons of global test accuracy (see Definition 2) in decentralized training of ResNet-18 on the CIFAR-100 dataset, distributed across 16 agents with high heterogeneity (Dirichlet  $\alpha = 0.1$ ; see details in Appendix C.1). Fully-connected communication (synchronous AllReduce) is activated only in specific windows, while low communication with one random peer with a probability of 0.2 is used elsewhere. **(a)**: Fully-connected communication in 1/10 of total rounds. **(b)**: Fully-connected communication in 1/20 of total rounds. In both, lighter bars show peak accuracy, darker bars show final accuracy. **(c)**: Global test accuracy curves for local models and the globally averaged model (counterfactual) under persistent low communication (blue) and no communication (orange).

To investigate this, we conduct experiments where fully-connected communication is applied only once, implemented by a single global merging. As shown in Figure 1a and Figure 1b, a single global merging is sufficient to significantly improve global generalization. Consistent gains by a single global merging are observed across a wide range of settings, including different datasets, model architectures, optimizers, initialization schemes, and communication topologies (see additional experimental results in Appendix C.2). The significant increase in generalization suggests that the generalization potential of decentralized learning might be considerably underestimated.

**Comparison with Chen et al. [11].** We note that Chen et al. [11] demonstrate the benefits of periodic global averaging in decentralized learning. However, our work differs in two key aspects: (1) *Communication cost*. Their method performs global averaging every  $H = 48$  steps, resulting in over 270 rounds of global communication. In contrast, we perform only *a single* global merging at the end of training. (2) *Research focus*. While both works share the goal of accelerating decentralized training through improved communication, our work offers a new perspective by studying why local models remain mergeable under extremely limited communication and high data heterogeneity.

### 4.3 Mergeability Persists under Limited but Nonzero Communication

A follow-up question is whether the effectiveness of the global merging is specific to the end of training. To investigate this, we assess the *counterfactual* performance of the globally averaged model at each training round, as depicted by the light-blue curve in Figure 3c.<sup>6</sup> The experiments are conducted under a lower-communication setting, where each agent communicates with one random peer at each round with probability 0.2 (see “Communication Graph” in Appendix C.1). A consistent superiority of the merged model (light-blue curve) over the local models (dark-blue curve) is observed throughout training, suggesting that local models remain mergeable at all stages (see Definition 1).

As an ablation, we conduct an experiment in which all models are trained entirely locally without any communication (see Figure 3c). In this case, the counterfactual test performance of the globally averaged model remains close to zero (light-orange curve), indicating that without communication, local models are not mergeable. This suggests that mergeability does *not* arise inherently from the local models themselves. Interestingly, under the low-communication setting, the test performance of local models before merging (dark-blue curve) remains similar to that in the no-communication case (dark-orange curve). However, after global merging, the resulting model shows significant generalization improvement. This clear contrast implies that extremely limited but nonzero communication plays a pivotal role in enabling mergeability.

<sup>6</sup>The term “counterfactual” refers to the fact that no global merging occurs during decentralized training. Instead, we manually compute the test accuracy of the hypothetical globally averaged model to quantify the “mergeability” of local models.

The counterfactual test performance of local models provides a lens to understand the surge-and-decline pattern observed in Figure 3. During the fully-connected communication phase, the local model effectively realizes the performance of the counterfactual globally merged model, resulting in a sharp increase in test accuracy. However, once the communication drops back to a limited setting, the performance returns back to that of the unmerged local models.

## 5 Theoretical Analysis

In this section, we examine the underlying mechanisms that enable the mergeability of local models in decentralized learning. As an initial step, we conduct a fine-grained convergence analysis of the globally merged models trained by Decentralized SGD (DSGD).<sup>7</sup> To substantiate the mergeability of local models, we compare the convergence rate of the merged model of DSGD model to that of a strong baseline—centralized mini-batch SGD (CSGD). Remarkably, we prove that the merged model in decentralized learning can converge to the optimum faster than its centralized counterpart. This suggests that the merged model not only preserves but may even surpass the performance of individual local models, thereby providing theoretical support for the mergeability (see Definition 1). While prior analyses regard the discrepancy among local models as purely detrimental, we show that part of this discrepancy, when coupled with the progressive sharpening of the loss landscape, can in fact accelerate convergence.

### 5.1 Assumptions

We start by introducing the commonly used assumptions from literature [43, 42].

**Assumption 1** (Mixing matrix). *Each sample of the (randomized) mixing matrix  $W \in \mathbb{R}^{m \times m}$  is doubly stochastic. Moreover, there exists  $p > 0$  such that*

$$\mathbb{E}_W \|\Theta W - \bar{\Theta}\|_F^2 \leq (1-p) \|\Theta - \bar{\Theta}\|_F^2, \quad \forall \Theta \in \mathbb{R}^{d \times m}. \quad (4)$$

Here  $\Theta = [\theta_1, \dots, \theta_m]$ ,  $\bar{\Theta} = [\bar{\theta}, \dots, \bar{\theta}] \equiv \Theta \frac{1}{m} \mathbf{1}\mathbf{1}^\top$  where  $\bar{\theta} = \frac{1}{m} \sum_{k=1}^m \theta_k$ .

**Assumption 2** ( $L$ -smoothness). *Each population risk  $\mathcal{L}_k = \mathbb{E}_{\xi_k \sim \mathcal{D}_k} \mathcal{L}(\theta; \xi_k)$  for  $k \in \{1, \dots, m\}$  is continuously differentiable, and there is a constant  $L \geq 0$  such that:*

$$\|\nabla \mathcal{L}_k(\theta) - \nabla \mathcal{L}_k(\vartheta)\| \leq L \|\theta - \vartheta\|, \quad \forall \theta, \vartheta \in \mathbb{R}^d. \quad (5)$$

**Assumption 3** (Bounded noise and diversity). *There exist  $\sigma^2, \zeta^2 \geq 0$  such that for any  $\theta_k \in \{\theta_k\}_{k=1}^m$ :*

$$\frac{1}{m} \sum_{k=1}^m \mathbb{E}_{\xi_k} \|\nabla \mathcal{L}_k(\theta_k; \xi_k) - \nabla \mathcal{L}_k(\theta_k)\|_2^2 \leq \sigma^2, \quad \frac{1}{m} \sum_{k=1}^m \|\nabla \mathcal{L}_k(\theta_k) - \nabla \mathcal{L}(\theta_k)\|_2^2 \leq \zeta^2, \quad (6)$$

where  $\mathcal{L}(\theta) = \frac{1}{m} \sum_{k=1}^m \mathcal{L}_k(\theta)$ .

### 5.2 Convergence Analysis

**Theorem 1** (Non-convex Convergence Rate of DSGD). *Suppose Assumption 2 and Assumption 3 hold. Consider decentralized SGD (DSGD) with a learning rate satisfying  $\eta \leq \frac{1}{L}$ , and let  $\bar{\theta}^{(t)} = \frac{1}{m} \sum_{k=1}^m \theta_k^{(t)}$  denote the averaged model at the  $t$ -th step. It holds that  $\frac{1}{T} \sum_{t=0}^{T-1} \mathbb{E} \left[ \|\nabla \mathcal{L}(\bar{\theta}^{(t)})\|_2^2 \right] \leq \varepsilon$ , After the total number of steps*

$$T = \mathcal{O} \left( \frac{\sigma^2}{m\varepsilon^2} + \frac{1}{\varepsilon} + \frac{1}{\varepsilon^2} \sum_t A^{(t)} \right) \cdot L(\mathcal{L}(\theta^{(0)}) - \mathcal{L}^*),$$

where  $A^{(t)} \triangleq \eta L (2T_2 + L_3^2 \Xi_t^4 + (2L_1 + 2L_3 \Xi_t^2 + \frac{mL_4^2}{24^2}) \sqrt{m} \Xi_t^3)$ . Here,  $T_2 = (\nabla^2 \mathcal{L}(\bar{\theta}^{(t)}) \Gamma^{(t)})^\top \nabla \text{Tr}(\nabla^2 \mathcal{L}(\bar{\theta}^{(t)}) \Gamma^{(t)})$ , and  $\Xi_t^2 = \text{Tr}(\Gamma^{(t)})$  with  $\Gamma^{(t)} = \frac{1}{m} \sum_{k=1}^m (\theta_k^{(t)} - \bar{\theta}^{(t)})(\theta_k^{(t)} - \bar{\theta}^{(t)})^\top$ . Constants  $L_1, L_3, L_4$  satisfy  $\|\nabla^q \mathcal{L}(\theta)\| \leq L_q$  for  $q = 1, 3, 4, \forall \theta$ .

<sup>7</sup>We note that while our theoretical analysis focuses on decentralized SGD, our main experiments employ decentralized AdamW, primarily due to its improved performance in Non-IID settings. To ensure the consistency between our theoretical analysis and empirical results, we also conduct experiments using decentralized SGD (see Appendix C.2).

Table 1: Comparison of non-convex convergence rates for centralized mini-batch SGD (CSGD) and decentralized SGD (DSGD) in non-iid settings.

Algorithm	CSGD ( $m$ agents)	DSGD [42]	DSGD (ours)
Rate	$\mathcal{O}\left(\frac{\sigma^2}{m\varepsilon^2} + \frac{1}{\varepsilon}\right)$	$\mathcal{O}\left(\frac{\sigma^2}{m\varepsilon^2} + \frac{1}{p\varepsilon} + \frac{\sqrt{p}\sigma + \zeta}{p\varepsilon^{3/2}}\right)$	$\mathcal{O}\left(\frac{\sigma^2}{m\varepsilon^2} + \frac{1}{\varepsilon} + \frac{1}{\varepsilon^2} \sum_t A^{(t)}\right)$

**Comparison.** As summarized in Table 1, Koloskova et al. [42] showed that DSGD suffers from additional terms of order  $\mathcal{O}\left(\frac{1-p}{p\varepsilon} + \frac{\sqrt{p}\sigma + \zeta}{p\varepsilon^{3/2}}\right)$  in the convergence rate compared to CSGD. The core idea behind their analysis is to separate the effects of three key factors: the descent force (i.e., the squared gradient norm), gradient noise, and parameter discrepancy among agents. Each of these components is then analyzed and controlled separately. Among them, both the gradient noise and the agent discrepancy are treated as detrimental to convergence. In contrast, we adopt a new proof framework that leverages the implicit bias of decentralized learning (see Proposition D.3 [109] and Appendix B.2). Rather than treating the discrepancy among agents purely as noise, we partially incorporate it as a constructive component that may accelerate convergence. This intuition is formalized through the convergence guarantee provided in Theorem 1, where the additional term takes the form  $\mathcal{O}\left(\frac{1}{\varepsilon^2} \sum_t A^{(t)}\right)$ . In what follows, we conduct a fine-grained analysis of the sign of  $A^{(t)}$ , in order to understand its precise role in driving convergence.

**Remark 1.** For the single-agent case where  $m = 1$ , we observe that  $A^{(t)} \equiv 0$  since  $\Xi_t \equiv 0$ . In this setting, Theorem 1 recovers the rate of standard SGD, which is of the order  $\mathcal{O}\left(\frac{\sigma^2}{\varepsilon^2} + \frac{1}{\varepsilon}\right)$ .

We introduce a new assumption for analyzing  $A^{(t)}$ , which is theoretically novel yet supported by empirical observations in deep learning in prior literature.

**Assumption 4** (Progressive sharpening). For any positive semi-definite matrix  $\Sigma$ , the gradient of population risk negatively aligns with the gradient of sharpness. Formally,  $\forall \theta \in \mathbb{R}^d$ ,

$$\nabla \mathcal{L}(\theta)^\top \nabla \text{Tr}(\nabla^2 \mathcal{L}(\theta) \Sigma) < 0. \quad (7)$$

**Remark 2.** Intuitively,  $\text{Tr}(\nabla^2 \mathcal{L}(\theta) \Sigma)$  can be interpreted as an ‘‘average sharpness’’ around  $\theta$ ; see similar metrics in [30, 109]. Assumption 4 reflects a widely observed phenomenon in deep learning: The loss gradient exhibits a negative correlation with the gradient of sharpness [90, 14, 12].

Assumption 4 ensures that the term  $T_2$  in  $A^{(t)}$  remains negative, serving as a descent component. In the following, we formally establish that  $T_2$  dominates the other terms in  $A^{(t)}$  when  $\Xi_t^2$  is sufficiently small, thereby ensuring that  $A^{(t)}$  remains non-positive and thus contributes to optimization.

**Proposition 2.** Suppose Assumption 4 holds and assume that the gradient norm satisfies  $\|\nabla \mathcal{L}(\theta^{(t)})\| \geq c_t > 0$  for positive constant  $c_t$ . Then, for any fixed  $m > 0$ , there exists a sufficiently small  $\Xi_t^2 > 0$ , where  $\Xi_t^2 = \text{Tr}(\Gamma^{(t)})$  with  $\Gamma^{(t)} = \frac{1}{m} \sum_{k=1}^m (\theta_k^{(t)} - \bar{\theta}^{(t)})(\theta_k^{(t)} - \bar{\theta}^{(t)})^\top$ , such that the inequality

$$A^{(t)} \triangleq \eta L \left( 2T_2 + L_3^2 \Xi_t^4 + (2L_1 + 2L_3 \Xi_t^2 + \frac{mL_4^2}{24^2}) \sqrt{m} \Xi_t^3 \right) \leq 0 \quad (8)$$

holds. Here  $T_2 = (\nabla \mathcal{L}(\bar{\theta}^{(t)}))^\top \nabla \text{Tr}(\nabla^2 \mathcal{L}(\bar{\theta}^{(t)}) \Gamma^{(t)})$  and constants  $L_1, L_3, L_4$  satisfy  $\|\nabla^q \mathcal{L}(\theta)\| \leq L_q$  for  $q = 1, 3, 4, \forall \theta$ .

This proposition highlights the critical role of  $\Xi_t = \sqrt{\text{Tr}(\Gamma^{(t)})}$ . According to Corollary D.2, the expectation of  $\Xi_t^2$  is upper bounded by

$$\mathbb{E}[\Xi_t^2] \leq \mathcal{O}\left((1-p)\eta^2 \left(\frac{\phi_{t-1}^2}{p^2} + \frac{\sigma^2}{p}\right)\right), \quad (9)$$

under a mild assumption that the gradient-norms change slowly, namely,  $\phi_t^2 \leq (1 + \frac{p}{4}) \phi_{t+1}^2$ , where  $\phi_t^2 = \frac{1}{m} \sum_{k=1}^m \|\nabla \mathcal{L}_k(\theta_k^{(t)})\|^2$ , and  $\mathcal{L}_k(\theta) = \mathbb{E}_{\xi_k \sim \mathcal{D}_k}[\mathcal{L}(\theta; \xi_k)]$ . The parameter  $p \in (0, 1]$  reflects the

level of connectivity in the communication graph (see [Assumption 1](#)). A larger  $p$  indicates better connectivity and faster consensus, while a smaller  $p$  implies a sparse communication graph (i.e., lower communication) and slower information propagation. For example,  $p = 1$  corresponds to a fully connected graph, enabling perfect communication, whereas  $p = 0$  represents the extreme case of local training with no communication.

**Remark 3.** For the fully-connected case where  $p = 1$ , we observe that  $A^{(t)} \equiv 0$  as  $\Xi_t \equiv 0$ . In this case, [Theorem 1](#) recovers the rate of standard SGD, where no acceleration effect is introduced.

**Why Limited but Nonzero Communication is Sufficient for Mergeability.** Notably, random communication graphs can achieve  $p = \Theta(1)$ , striking a favorable trade-off: they require relatively low communication overhead while still maintaining efficient information mixing due to randomized edge sampling, which ensures rapid consensus [88]. This is why we adopt random topologies as the primary setup in our experiments—they can satisfy the condition in [Proposition 2](#) even under extremely limited communication, thereby ensuring that mergeability (see [Figure 1](#)).

However, in the case of full local training where  $p = 0$  (see [Figure 2](#)), the right-hand side of [Equation \(9\)](#) diverges to infinity, indicating that  $\Xi_t$  becomes unbounded. As a consequence, the condition of  $A^{(t)}$  in [Proposition 2](#) can no longer be satisfied, which explains why local models after full local training may not be reliably merged.

### 5.3 A Sufficient Condition for Acceleration

We further provide a sufficient condition for acceleration (i.e., [Equation \(8\)](#) holds):

**Proposition 3** (Critical Consensus Edge). *Suppose that the gradient-norms change slowly, i.e.,  $\phi_t^2 \leq (1 + \frac{p}{4}) \phi_{t+1}^2$ , where  $\phi_t^2 = \frac{1}{m} \sum_{k=1}^m \|\nabla \mathcal{L}_k(\theta_k^{(t)})\|^2$ , and  $\mathcal{L}_k(\theta) = \mathbb{E}_{\xi_k \sim \mathcal{D}_k} [\mathcal{L}(\theta; \xi_k)]$ . The following condition is sufficient for ensuring that [Equation \(8\)](#) holds.*

$$24(1-p)\eta^2 \left( \frac{\phi_{t-1}^2}{p^2} + \frac{\sigma^2}{p} \right) < \min \left\{ \sqrt{\frac{\gamma c_t}{2L_3^2}}, \frac{\gamma c_t}{\left(2L_1 + \frac{\gamma c_t}{L_3} + \frac{mL_4^2}{24^2}\right) \sqrt{m}} \right\}, \quad (10)$$

where  $\gamma$  is the relative degree of progressive sharpening (see [Assumption 4](#) and [Equation \(D.11\)](#)), and  $c_t$  is the lower bound on the gradient norm satisfying  $\|\nabla \mathcal{L}(\bar{\theta}^{(t)})\| \geq c_t > 0$ . Constants  $L_1, L_3, L_4$  satisfy  $\|\nabla^q \mathcal{L}(\theta)\| \leq L_q$  for  $q = 1, 3, 4, \forall \theta$ .

**Practical Implications.** This condition offers useful insights into how communication should be allocated over training to balance performance and communication cost. Specifically,

- In the early stages of training, the gradient norm lower bound  $c_t$  is large, allowing the right-hand side of [Equation \(10\)](#) to tolerate larger consensus error. This permits low-frequency communication (i.e., smaller  $p$ ) without significantly impacting convergence.
- As training progresses and the gradient norm  $c_t$  decreases, the bound becomes tighter, which necessitates more frequent communication (i.e., larger  $p$ ).

We note that this aligns perfectly with our empirical findings in [Section 4](#), reinforcing one of our key empirical observations: More communication should be concentrated in the later stages of training.

## 6 Conclusion

In this paper, we study how to allocate communication over temporal levels in decentralized learning. Empirical results show that concentrating communication in the later stages significantly improves global generalization, and remarkably, a single global merging at the end of training suffices to recover server-based learning performance. Moreover, we show that local models remain mergeable under limited yet nonzero communication throughout training. To explain these empirical findings, we provide a theoretical guarantee showing that the merged model can even outperform centralized mini-batch SGD. Our empirical and theoretical results challenge the conventional belief that decentralized learning fails to generalize well under data heterogeneity and low communication, offering new insights into both model merging and communication-efficient decentralized learning.

## References

- [1] Ainsworth, S., Hayase, J., and Srinivasa, S. (2023). Git re-basin: Merging models modulo permutation symmetries. In *The Eleventh International Conference on Learning Representations*.
- [2] Allouah, Y., Koloskova, A., Firdoussi, A. E., Jaggi, M., and Guerraoui, R. (2024). The privacy power of correlated noise in decentralized learning. In *Proceedings of the 41st International Conference on Machine Learning*, volume 235, pages 1115–1143.
- [3] Bonabeau, E., Dorigo, M., and Theraulaz, G. (1999). *Swarm Intelligence: From Natural to Artificial Systems*. Oxford University Press.
- [4] Bornstein, M., Rabbani, T., Wang, E. Z., Bedi, A., and Huang, F. (2023). SWIFT: Rapid decentralized federated learning via wait-free model communication. In *The Eleventh International Conference on Learning Representations*.
- [5] Borzunov, A., Baranchuk, D., Dettmers, T., Riabinin, M., Belkada, Y., Chumachenko, A., Samygin, P., and Raffel, C. (2023a). Petals: Collaborative inference and fine-tuning of large models. In *Proceedings of the 61st Annual Meeting of the Association for Computational Linguistics (Volume 3: System Demonstrations)*, pages 558–568. Association for Computational Linguistics.
- [6] Borzunov, A., Ryabinin, M., Chumachenko, A., Baranchuk, D., Dettmers, T., Belkada, Y., Samygin, P., and Raffel, C. A. (2023b). Distributed inference and fine-tuning of large language models over the internet. In *Advances in Neural Information Processing Systems*.
- [7] Cao, Y., Wu, Z., Yuan, K., and Sayed, A. H. (2024). On the trade-off between flatness and optimization in distributed learning. *arXiv preprint arXiv:2406.20006*.
- [8] CCAF (2023). Cambridge bitcoin electricity consumption index (CBECI). <https://ccaf.io/cbnsi/cbeci>.
- [9] Chen, L., Ye, H., and Luo, L. (2024). An efficient stochastic algorithm for decentralized nonconvex-strongly-concave minimax optimization. *International Conference on Artificial Intelligence and Statistics*.
- [10] Chen, X., Huang, M., Ma, S., and Balasubramanian, K. (2023). Decentralized stochastic bilevel optimization with improved per-iteration complexity. In *Proceedings of the 40th International Conference on Machine Learning*, volume 202, pages 4641–4671. PMLR.
- [11] Chen, Y., Yuan, K., Zhang, Y., Pan, P., Xu, Y., and Yin, W. (2021). Accelerating gossip sgd with periodic global averaging. In *Proceedings of the 38th International Conference on Machine Learning*, volume 139, pages 1791–1802. PMLR.
- [12] Cohen, J. M., Damian, A., Talwalkar, A., Kolter, Z., and Lee, J. D. (2025). Understanding optimization in deep learning with central flows. In *The Thirteenth International Conference on Learning Representations*.
- [13] Cyffers, E., Bellet, A., and Upadhyay, J. (2024). Differentially private decentralized learning with random walks. In *Proceedings of the 41st International Conference on Machine Learning*, volume 235, pages 9762–9783.
- [14] Damian, A., Nichani, E., and Lee, J. D. (2023). Self-stabilization: The implicit bias of gradient descent at the edge of stability. In *the Eleventh International Conference on Learning Representations*.
- [15] Dekel, O., Gilad-Bachrach, R., Shamir, O., and Xiao, L. (2012). Optimal distributed online prediction using mini-batches. *Journal of Machine Learning Research*, 13(6):165–202.
- [16] Douillard, A., Feng, Q., Rusu, A. A., Chhaparia, R., Donchev, Y., Kuncoro, A., Ranzato, M., Szlam, A., and Shen, J. (2023). Diloco: Distributed low-communication training of language models. *arXiv preprint arXiv:2311.08105*.
- [17] Draxler, F., Veschgini, K., Salmhofer, M., and Hamprecht, F. (2018). Essentially no barriers in neural network energy landscape. In *International conference on machine learning*, pages 1309–1318. PMLR.

- [18] Entezari, R., Sedghi, H., Saukh, O., and Neyshabur, B. (2022). The role of permutation invariance in linear mode connectivity of neural networks. In *International Conference on Learning Representations*.
- [19] Even, M., Koloskova, A., and Massoulié, L. (2024). Asynchronous SGD on graphs: a unified framework for asynchronous decentralized and federated optimization. In *Proceedings of the 27th International Conference on Artificial Intelligence and Statistics*.
- [20] Fort, S., Dziugaite, G. K., Paul, M., Kharaghani, S., Roy, D. M., and Ganguli, S. (2020). Deep learning versus kernel learning: an empirical study of loss landscape geometry and the time evolution of the neural tangent kernel. *Advances in Neural Information Processing Systems*, 33:5850–5861.
- [21] Frankle, J., Dziugaite, G. K., Roy, D., and Carbin, M. (2020). Linear mode connectivity and the lottery ticket hypothesis. In *International Conference on Machine Learning*, pages 3259–3269. PMLR.
- [22] Freeman, C. D. and Bruna, J. (2017). Topology and geometry of half-rectified network optimization. In *International Conference on Learning Representations*.
- [23] Gao, H., Gu, B., and Thai, M. T. (2023). On the convergence of distributed stochastic bilevel optimization algorithms over a network. In *Proceedings of The 26th International Conference on Artificial Intelligence and Statistics*, volume 206, pages 9238–9281. PMLR.
- [24] Gao, H. and Huang, H. (2021). Fast training method for stochastic compositional optimization problems. *Advances in Neural Information Processing Systems*, 34:25334–25345.
- [25] Gardizy, A. and Efrati, A. (2024). Microsoft and OpenAI plot \$100 billion stargate AI super-computer. *The Information*.
- [26] Garipov, T., Izmailov, P., Podoprikin, D., Vetrov, D. P., and Wilson, A. G. (2018). Loss surfaces, mode connectivity, and fast ensembling of dnns. *Advances in neural information processing systems*, 31.
- [27] Grand View Research (2024). Ai infrastructure market size, share & growth report, 2030.
- [28] Gu, X., Lyu, K., Arora, S., Zhang, J., and Huang, L. (2024). A quadratic synchronization rule for distributed deep learning. In *The Twelfth International Conference on Learning Representations*.
- [29] Gu, X., Lyu, K., Huang, L., and Arora, S. (2023a). Why (and when) does local SGD generalize better than SGD? In *International Conference on Learning Representations*.
- [30] Gu, X., Lyu, K., Huang, L., and Arora, S. (2023b). Why (and when) does local SGD generalize better than SGD? In *The Eleventh International Conference on Learning Representations*.
- [31] Gurbuzbalaban, M., Hu, Y., Simsekli, U., Yuan, K., and Zhu, L. (2022). Heavy-tail phenomenon in decentralized sgd. *arXiv preprint arXiv:2205.06689*.
- [32] He, F., Nan, L., and Zhu, T. (2025). Imagining a democratic, affordable future of foundation models: A decentralised avenue. In *Handbook of Blockchain Analytics*. Springer.
- [33] He, K., Zhang, X., Ren, S., and Sun, J. (2016). Identity mappings in deep residual networks. In *European conference on computer vision*.
- [34] He, L., Karimireddy, S. P., and Jaggi, M. (2022). Byzantine-robust decentralized learning via clippedgossip. *arXiv preprint arXiv:2202.01545*.
- [35] Hsu, T.-M. H., Qi, H., and Brown, M. (2019). Measuring the effects of non-identical data distribution for federated visual classification. *arXiv preprint arXiv:1909.06335*.
- [36] Ilharco, G., Ribeiro, M. T., Wortsman, M., Schmidt, L., Hajishirzi, H., and Farhadi, A. (2023). Editing models with task arithmetic. In *The Eleventh International Conference on Learning Representations*.

- [37] Ilharco, G., Wortsman, M., Gadre, S. Y., Song, S., Hajishirzi, H., Kornblith, S., Farhadi, A., and Schmidt, L. (2022). Patching open-vocabulary models by interpolating weights. In Oh, A. H., Agarwal, A., Belgrave, D., and Cho, K., editors, *Advances in Neural Information Processing Systems*.
- [38] Izmailov, P., Podoprikin, D., Garipov, T., Vetrov, D. P., and Wilson, A. G. (2018). Averaging weights leads to wider optima and better generalization. In Globerson, A. and Silva, R., editors, *Proceedings of the Thirty-Fourth Conference on Uncertainty in Artificial Intelligence, UAI 2018, Monterey, California, USA, August 6-10, 2018*, pages 876–885. AUAI Press.
- [39] Jaghouar, S., Ong, J. M., Basra, M., Obeid, F., Straube, J., Keiblinger, M., Bakouch, E., Atkins, L., Panahi, M., Goddard, C., et al. (2024). Intellect-1 technical report. *arXiv preprint arXiv:2412.01152*.
- [40] Kharrat, S., Canini, M., and Horvath, S. (2024). Decentralized personalized federated learning. *arXiv preprint arXiv:2406.06520*.
- [41] Kolehmainen, J., Blagoev, N., Donaghy, J., Ersoy, O., and Nies, C. (2025). Noloco: No-all-reduce low communication training method for large models. *arXiv preprint arXiv:2506.10911*.
- [42] Koloskova, A., Loizou, N., Boreiri, S., Jaggi, M., and Stich, S. (2020). A unified theory of decentralized SGD with changing topology and local updates. In *International Conference on Machine Learning*.
- [43] Kong, L., Lin, T., Koloskova, A., Jaggi, M., and Stich, S. (2021a). Consensus control for decentralized deep learning. In *International Conference on Machine Learning*. PMLR.
- [44] Kong, L., Lin, T., Koloskova, A., Jaggi, M., and Stich, S. (2021b). Consensus control for decentralized deep learning. In *Proceedings of the 38th International Conference on Machine Learning*.
- [45] Krizhevsky, A., Hinton, G., et al. (2009). Learning multiple layers of features from tiny images (tech. rep.). *University of Toronto*.
- [46] Le, Y. and Yang, X. (2015). Tiny imagenet visual recognition challenge. *CS 231N*.
- [47] Le Bars, B., Bellet, A., Tommasi, M., Lavoie, E., and Kermarrec, A.-M. (2023). Refined convergence and topology learning for decentralized sgd with heterogeneous data. In *Proceedings of the 26th International Conference on Artificial Intelligence and Statistics*.
- [48] Le Bars, B., Bellet, A., Tommasi, M., Scaman, K., and Neglia, G. (2024). Improved stability and generalization guarantees of the decentralized SGD algorithm. In *Proceedings of the 41st International Conference on Machine Learning*.
- [49] Li, M., Andersen, D. G., Smola, A. J., and Yu, K. (2014). Communication efficient distributed machine learning with the parameter server. *Advances in Neural Information Processing Systems*.
- [50] Li, M., Gururangan, S., Dettmers, T., Lewis, M., Althoff, T., Smith, N. A., and Zettlemoyer, L. (2022a). Branch-train-merge: Embarrassingly parallel training of expert language models. In *First Workshop on Interpolation Regularizers and Beyond at NeurIPS 2022*.
- [51] Li, S., Zhou, T., Tian, X., and Tao, D. (2022b). Learning to collaborate in decentralized learning of personalized models. In *Proceedings of the IEEE/CVF Conference on Computer Vision and Pattern Recognition (CVPR)*, pages 9766–9775.
- [52] Li, Z., Wang, T., and Arora, S. (2022c). What happens after SGD reaches zero loss? –a mathematical framework. In *International Conference on Learning Representations*.
- [53] Lian, X., Zhang, C., Zhang, H., Hsieh, C.-J., Zhang, W., and Liu, J. (2017). Can decentralized algorithms outperform centralized algorithms? a case study for decentralized parallel stochastic gradient descent. In *Advances in Neural Information Processing Systems*.
- [54] Lian, X., Zhang, W., Zhang, C., and Liu, J. (2018). Asynchronous decentralized parallel stochastic gradient descent. In *International Conference on Machine Learning*.

- [55] Lin, T., Karimireddy, S. P., Stich, S., and Jaggi, M. (2021). Quasi-global momentum: Accelerating decentralized deep learning on heterogeneous data. In *Proceedings of the 38th International Conference on Machine Learning*.
- [56] Lu, Y. and De Sa, C. (2021). Optimal complexity in decentralized training. In *Proceedings of the 38th International Conference on Machine Learning*.
- [57] Lyu, K. (2024). *Implicit Bias of Deep Learning Optimization: A Mathematical Examination*. PhD thesis, Princeton University.
- [58] Martínez Beltrán, E. T., Pérez, M. Q., Sánchez, P. M. S., Bernal, S. L., Bovet, G., Pérez, M. G., Pérez, G. M., and Celdrán, A. H. (2023). Decentralized federated learning: Fundamentals, state of the art, frameworks, trends, and challenges. *IEEE Communications Surveys & Tutorials*, 25(4):2983–3013.
- [59] Matena, M. S. and Raffel, C. (2022). Merging models with fisher-weighted averaging. In Oh, A. H., Agarwal, A., Belgrave, D., and Cho, K., editors, *Advances in Neural Information Processing Systems*.
- [60] Mavrouniotis, M., Li, C., and Yang, S. (2017). A survey of swarm intelligence for dynamic optimization: Algorithms and applications. *Swarm and Evolutionary Computation*, 33:1–17.
- [61] Mrini, A. E., Cyffers, E., and Bellet, A. (2024). Privacy attacks in decentralized learning. In *Proceedings of the 41st International Conference on Machine Learning*.
- [62] Nadiradze, G., Sabour, A., Davies, P., Li, S., and Alistarh, D. (2021). Asynchronous decentralized sgd with quantized and local updates. *Advances in Neural Information Processing Systems*.
- [63] Nagarajan, V. and Kolter, J. Z. (2019). Uniform convergence may be unable to explain generalization in deep learning. *Advances in Neural Information Processing Systems*, 32.
- [64] Nedić, A. and Olshevsky, A. (2014). Distributed optimization over time-varying directed graphs. volume 60, pages 601–615. IEEE.
- [65] Nedic, A. and Ozdaglar, A. (2009). Distributed subgradient methods for multi-agent optimization. *IEEE Transactions on Automatic Control*, 54(1):48–61.
- [66] OpenAI (2025). Announcing the stargate project. <https://openai.com/index/announcing-the-stargate-project/>.
- [67] Ortiz-Jimenez, G., Favero, A., and Frossard, P. (2023). Task arithmetic in the tangent space: Improved editing of pre-trained models. In *Thirty-seventh Conference on Neural Information Processing Systems*.
- [68] Pilz, K. F., Sanders, J., Rahman, R., and Heim, L. (2025). Trends in ai supercomputers. *arXiv preprint arXiv:2504.16026*.
- [69] Radford, A., Kim, J. W., Hallacy, C., Ramesh, A., Goh, G., Agarwal, S., Sastry, G., Askell, A., Mishkin, P., Clark, J., Krueger, G., and Sutskever, I. (2021). Learning transferable visual models from natural language supervision. In Meila, M. and Zhang, T., editors, *Proceedings of the 38th International Conference on Machine Learning*, volume 139 of *Proceedings of Machine Learning Research*, pages 8748–8763. PMLR.
- [70] Ramasinghe, S., Ajanthan, T., Avraham, G., Zuo, Y., and Long, A. (2025). Protocol models: Scaling decentralized training with communication-efficient model parallelism. *arXiv preprint arXiv:2506.01260*.
- [71] Rame, A., Ahuja, K., Zhang, J., Cord, M., Bottou, L., and Lopez-Paz, D. (2023). Model ratatouille: Recycling diverse models for out-of-distribution generalization. In Krause, A., Brunskill, E., Cho, K., Engelhardt, B., Sabato, S., and Scarlett, J., editors, *Proceedings of the 40th International Conference on Machine Learning*, volume 202 of *Proceedings of Machine Learning Research*, pages 28656–28679. PMLR.

- [72] Rame, A., Kirchmeyer, M., Rahier, T., Rakotomamonjy, A., patrick gallinari, and Cord, M. (2022). Diverse weight averaging for out-of-distribution generalization. In Oh, A. H., Agarwal, A., Belgrave, D., and Cho, K., editors, *Advances in Neural Information Processing Systems*.
- [73] Richards, D. et al. (2020). Graph-dependent implicit regularisation for distributed stochastic subgradient descent. *Journal of Machine Learning Research*.
- [74] Ryabinin, M., Dettmers, T., Diskin, M., and Borzunov, A. (2023). SWARM parallelism: Training large models can be surprisingly communication-efficient. In *Proceedings of the 40th International Conference on Machine Learning*, volume 202 of *Proceedings of Machine Learning Research*, pages 29416–29440. PMLR.
- [75] Sayed, A. H. (2014). *Adaptation, Learning, and Optimization over Networks*. Now Publishers.
- [76] Sergeev, A. and Del Balso, M. (2018). Horovod: fast and easy distributed deep learning in tensorflow. *arXiv preprint arXiv:1802.05799*.
- [77] Shen, L., Sun, Y., Yu, Z., Ding, L., Tian, X., and Tao, D. (2024). On efficient training of large-scale deep learning models. *ACM Computing Surveys*, 57(3).
- [78] Shen, T., Zhu, D., Zhao, Z., Wu, C., and Wu, F. (2025). Will llms scaling hit the wall? breaking barriers via distributed resources on massive edge devices. *arXiv preprint arXiv:2503.08223*.
- [79] Singha, A., Lua, C., Gupta, G., Chopra, A., Blanca, J., Klinghoffer, T., Tiwary, K., and Raskara, R. (2024). A perspective on decentralizing ai.
- [80] Sonthalia, A., Rubinstein, A., Abbasnejad, E., and Oh, S. J. (2025). Do deep neural network solutions form a star domain? In *The Thirteenth International Conference on Learning Representations*.
- [81] Sun, T., Li, D., and Wang, B. (2021). Stability and generalization of decentralized stochastic gradient descent. In *Proceedings of the AAAI Conference on Artificial Intelligence*.
- [82] Takezawa, Y., Sato, R., Bao, H., Niwa, K., and Yamada, M. (2023). Beyond exponential graph: Communication-efficient topologies for decentralized learning via finite-time convergence. In *Thirty-seventh Conference on Neural Information Processing Systems*.
- [83] Tang, H., Lian, X., Yan, M., Zhang, C., and Liu, J. (2018). D2: Decentralized training over decentralized data. In *International Conference on Machine Learning*. PMLR.
- [84] Tsitsiklis, J., Bertsekas, D., and Athans, M. (1986). Distributed asynchronous deterministic and stochastic gradient optimization algorithms. *IEEE Transactions on Automatic Control*, 31(9):803–812.
- [85] Vardi, G. (2023). On the implicit bias in deep-learning algorithms. *Commun. ACM*, 66(6):86–93.
- [86] Vogels, T., He, L., Koloskova, A., Karimireddy, S. P., Lin, T., Stich, S. U., and Jaggi, M. (2021). Relaysum for decentralized deep learning on heterogeneous data. In Beygelzimer, A., Dauphin, Y., Liang, P., and Vaughan, J. W., editors, *Advances in Neural Information Processing Systems*.
- [87] Vogels, T., Hendrikx, H., and Jaggi, M. (2023). Beyond spectral gap: The role of the topology in decentralized learning. *Journal of Machine Learning Research*, 24(355):1–31.
- [88] Vos, M. D., Farhadkhani, S., Guerraoui, R., marie Kermarrec, A., Pires, R., and Sharma, R. (2023). Epidemic learning: Boosting decentralized learning with randomized communication. In *Thirty-seventh Conference on Neural Information Processing Systems*.
- [89] Wang, J., Lu, Y., Yuan, B., Chen, B., Liang, P., De Sa, C., Re, C., and Zhang, C. (2023). CocktailSGD: Fine-tuning foundation models over 500Mbps networks. In *Proceedings of the 40th International Conference on Machine Learning*, volume 202 of *Proceedings of Machine Learning Research*, pages 36058–36076. PMLR.
- [90] Wang, Z., Li, Z., and Li, J. (2022). Analyzing sharpness along GD trajectory: Progressive sharpening and edge of stability. In Oh, A. H., Agarwal, A., Belgrave, D., and Cho, K., editors, *Advances in Neural Information Processing Systems*.

- [91] Wortsman, M., Ilharco, G., Gadre, S. Y., Roelofs, R., Gontijo-Lopes, R., Morcos, A. S., Namkoong, H., Farhadi, A., Carmon, Y., Kornblith, S., et al. (2022a). Model soups: averaging weights of multiple fine-tuned models improves accuracy without increasing inference time. In *International Conference on Machine Learning*, pages 23965–23998. PMLR.
- [92] Wortsman, M., Ilharco, G., Kim, J. W., Li, M., Kornblith, S., Roelofs, R., Lopes, R. G., Hajishirzi, H., Farhadi, A., Namkoong, H., and Schmidt, L. (2022b). Robust fine-tuning of zero-shot models. In *Proceedings of the IEEE/CVF Conference on Computer Vision and Pattern Recognition (CVPR)*, pages 7959–7971.
- [93] Wu, T. and Sun, Y. (2024). Implicit regularization of decentralized gradient descent for sparse regression. In *the Thirty-eighth Annual Conference on Neural Information Processing Systems*.
- [94] Xian, W., Huang, F., Zhang, Y., and Huang, H. (2021). A faster decentralized algorithm for nonconvex minimax problems. *Advances in Neural Information Processing Systems*, 34:25865–25877.
- [95] Xu, J., Zhang, W., and Wang, F. (2021). A(dp)<sup>2</sup>sgd: Asynchronous decentralized parallel stochastic gradient descent with differential privacy. *IEEE Transactions on Pattern Analysis and Machine Intelligence*.
- [96] Yadav, P., Tam, D., Choshen, L., Raffel, C., and Bansal, M. (2023). TIES-merging: Resolving interference when merging models. In *Thirty-seventh Conference on Neural Information Processing Systems*.
- [97] Yang, S., Zhang, X., and Wang, M. (2022). Decentralized gossip-based stochastic bilevel optimization over communication networks. *Advances in Neural Information Processing Systems*, 35:238–252.
- [98] Ye, H. and Ling, Q. (2025). Generalization error matters in decentralized learning under Byzantine attacks. *IEEE Transactions on Signal Processing*.
- [99] Ying, B., Yuan, K., Chen, Y., Hu, H., Pan, P., and Yin, W. (2021). Exponential graph is provably efficient for decentralized deep training. In *Advances in Neural Information Processing Systems*.
- [100] Yuan, B., He, Y., Davis, J. Q., Zhang, T., Dao, T., Chen, B., Liang, P., Re, C., and Zhang, C. (2022). Decentralized training of foundation models in heterogeneous environments. *Advances in Neural Information Processing Systems*.
- [101] Yuan, K., Ling, Q., and Yin, W. (2016). On the convergence of decentralized gradient descent. *SIAM Journal on Optimization*, 26(3):1835–1854.
- [102] Yuan, L., Wang, Z., Sun, L., Yu, P. S., and Brinton, C. G. (2024). Decentralized federated learning: A survey and perspective. *IEEE Internet of Things Journal*, pages 1–1.
- [103] Yurochkin, M., Agarwal, M., Ghosh, S., Greenewald, K., Hoang, N., and Khazaeni, Y. (2019). Bayesian nonparametric federated learning of neural networks. In *Proceedings of the 36th International Conference on Machine Learning*.
- [104] Zehtabi, S., Han, D.-J., Parasnis, R., Hosseinalipour, S., and Brinton, C. G. (2025). Decentralized sporadic federated learning: A unified algorithmic framework with convergence guarantees. In *The Thirteenth International Conference on Learning Representations*.
- [105] Zhang, W., Liu, M., Feng, Y., Cui, X., Kingsbury, B., and Tu, Y. (2021). Loss landscape dependent self-adjusting learning rates in decentralized stochastic gradient descent. *arXiv preprint arXiv:2112.01433*.
- [106] Zhou, Z., Wang, M., Mao, Y., Li, B., and Yan, J. (2025). Sharpness-aware minimization efficiently selects flatter minima late in training. In *The Thirteenth International Conference on Learning Representations*.
- [107] Zhou, Z., Yang, Y., Yang, X., Yan, J., and Hu, W. (2023). Going beyond linear mode connectivity: The layerwise linear feature connectivity. In *Thirty-seventh Conference on Neural Information Processing Systems*.

- [108] Zhu, M., Shen, L., Du, B., and Tao, D. (2023a). Stability and generalization of the decentralized stochastic gradient descent ascent algorithm. In *Thirty-seventh Conference on Neural Information Processing Systems*.
- [109] Zhu, T., He, F., Chen, K., Song, M., and Tao, D. (2023b). Decentralized SGD and average-direction SAM are asymptotically equivalent. In *Proceedings of the 40th International Conference on Machine Learning*.
- [110] Zhu, T., He, F., Zhang, L., Niu, Z., Song, M., and Tao, D. (2022). Topology-aware generalization of decentralized SGD. In *International Conference on Machine Learning*. PMLR.
- [111] Zhu, T., Li, W., Wang, C., and He, F. (2025). DICE: Data influence cascade in decentralized learning. In *The Thirteenth International Conference on Learning Representations*.

## Impact Statement

This paper studies the problem of temporal communication allocation in decentralized distributed learning, a topic of increasing practical significance in the era of communication-intensive large model training. Specifically, we aim to contribute to the development of communication-efficient decentralized learning without compromising performance. The broader societal impact of our work lies in the potential democratization of access to large-scale distributed training. By reducing communication overhead, our approach lowers the communication resource requirements (e.g., bandwidth and synchronization latency) associated with decentralized learning. This makes it feasible for individuals or organizations with constrained infrastructure to participate in collaborative training. Such inclusivity can extend the applicability of distributed learning systems to edge environments, thereby promoting more equitable contributions to and usage of models trained at scale. No negative societal impacts are identified.

## A Potential Q&A

*Q: The empirical phenomena are observed under decentralized AdamW, while the theoretical analysis is based on decentralized DSGD.*

**A:** While our theoretical analysis is based on decentralized SGD, we use decentralized AdamW in the experiments due to its superior performance in Non-IID scenarios. To verify that this choice does not compromise the validity of our conclusions, we additionally conduct experiments with decentralized SGD, which yield consistent results and further support our claims (see [Appendix C.2](#)).

*Q: How does theory part explain "local models in decentralized learning are globally mergeable"?*

**A:** The theoretical explanation of the "mergeability" of local models in decentralized learning is supported by the result that a globally merged model converges faster to the optimum than the individual local models. Specifically, we provide a fine-grained convergence analysis showing that the merged model trained via Decentralized SGD (DSGD) can outperform centralized mini-batch SGD (CSGD), despite using limited communication. This suggests that the merged model not only preserves, but may even surpass, the performance of local models trained independently without merging, thereby providing theoretical support for their mergeability.

*Q: How the baselines were tuned in terms of hyperparameter?*

**A:** We tuned the hyperparameters via grid search. For example, for ResNet-18 trained from scratch on Tiny ImageNet, we searched the learning rate over the range  $[1 \times 10^{-4}, 5 \times 10^{-4}, 1 \times 10^{-3}]$  and the batch size from 64 to 128, selecting the configuration that yielded the best test performance. Importantly, the main observations remain consistent across a wide range of learning rates and batch sizes, demonstrating the robustness of our findings (see hyperparameter setup in [Appendix C.1](#) and results in [Appendix C.2](#)).

*Q: How does different or same initialization affect results?*

**A:** Most of our experiments are conducted for models with different initializations. Even starting from different points, the local models can still be merged with limited communications during training. We also conduct experiments with pretraining (see [Figure 1a](#) and [Appendix C.2](#)). We note that consistent gains of single global merging are observed across different initialization schemes.

## B Additional Background and Related Work

### B.1 Decentralized Learning

Modern large-scale model training and inference are predominantly conducted within centralized, high-cost data centers. Driven by mounting constraints on computational resources and power availability [68], both academia and industry are increasingly exploring decentralized training approaches [66, 27]. This paradigm, drawing inspiration from swarm intelligence systems [3, 60], offers a more economical and scalable approach by distributing computational tasks across globally distributed nodes, rather than relying solely on a single central server [100, 6, 39, 70]. A notable illustration of the computational potential through decentralization is the Bitcoin system, which sustains work-

loads equivalent to a 16 GW power draw [8], surpassing by a factor of three the estimated 5 GW consumption of the largest AI supercluster under development [25, 66].

To provide context, we summarize key algorithmic and theoretical advances in decentralized learning. While our discussion highlights several notable contributions, it is not exhaustive; readers are referred to recent advances and surveys [111, 58, 79, 102, 32, 70, 41].

**Algorithmic Progress in Decentralized Learning.** The advancement of decentralized learning algorithms has been primarily driven by the need for communication-efficiency in practical distributed learning. Decentralized algorithms have been refined to handle a variety of realistic scenarios, including time-varying communication topologies [64, 42, 99, 82], asynchronous updates [54, 95, 62, 4, 19], statistical heterogeneity [83, 86, 47], and robustness to Byzantine failures [34, 98]. Moreover, recent works extend beyond standard empirical risk minimization to more structured problem classes, such as compositional [24], minimax [94, 108, 9], and bi-level optimization [97, 23, 10]. Additionally, privacy concerns in decentralized learning are also critical, with efforts focusing on differentially privacy [13, 2] and data reconstruction attacks [61].

**Theoretical Progress in Decentralized Learning.** Foundational work on decentralized optimization [65, 75, 101, 53] lay the groundwork for understanding convergence. Building on this, Lu and De Sa [56] propose a hierarchical abstraction of decentralization, distinguishing it into three layers, providing a unified view across federated and decentralized paradigms. Koloskova et al. [42] consolidate synchronous decentralized SGD algorithms with changing communication topologies and local updates, and Even et al. [19] extend the unifying perspective to asynchronous protocols. More recently, Zehtabi et al. [104] develop these frameworks further by considering the sporadicity of both communications and computations. On the generalization front, Richards et al. [73] derive stability-based bounds for decentralized SGD in convex settings, while Sun et al. [81] extend these to non-convex objectives, revealing a dependency on the spectral gap of the communication graph. This dependency was subsequently refined by Zhu et al. [110], who introduce a Gaussian weight difference assumption to tight the bound. Complementary results show that in convex regimes, the generalization of decentralized SGD matches that of centralized SGD [48], while in non-convex landscapes, decentralization primarily impacts worst-case generalization behavior. To account for unexplained generalization behaviors in decentralized training [44, 31, 87], Zhu et al. [109] link decentralized SGD to random sharpness-aware minimization (SAM), revealing a bias toward flatter minima. Notably, akin to our finding that decentralized learning generalizes when allocated high communications late in training, Zhou et al. [106] showed that SAM efficiently selects flatter minima when applied in the later stage of training.

**Towards Decentralized Training of Foundation Models.** Recent advances have shown the feasibility of training large-scale foundation models in decentralized environments. DT-FM [100] introduces tasklet-based scheduling for Transformer training under bandwidth-constrained settings, enabling efficient resource allocation. SWARM Parallelism [74] scales decentralized training through resilient pipeline design and adaptive load balancing. CocktailSGD [89] further improves efficiency via a combination of decentralization, gradient sparsification, and quantization for LLM fine-tuning. On the inference side, Petal [5] exploits peer-to-peer networks to amortize computational costs across heterogeneous nodes. Most recently, Intellect [39], building on Diloco [16], leverages hybrid parallelism, i.e., both data and model parallelism, to collaboratively train models with billions of parameters. NoLoCo [41] further extends Diloco to gossip-type decentralized settings. For a broad survey of large-scale deep learning practice, see Shen et al. [77, 78].

## B.2 Implicit Bias of Decentralized Learning

The concept of implicit bias—the intrinsic preference of learning algorithms for solutions with certain properties—has emerged as a key concept in explaining the empirical success of modern deep learning [52, 85, 57]. Recent studies have highlighted intriguing distinctions between decentralized stochastic gradient descent (DSGD) and its centralized counterpart (CSGD). Gurbuzbalaban et al. [31] demonstrate that under certain conditions, DSGD operating on large, sparse topologies exhibits heavier-tailed parameter distributions compared to CSGD. Zhang et al. [105] show that decentralization introduces a landscape-dependent noise, which can improve tolerance to larger learning rates. This observation aligns with findings by Vogels et al. [87], who reveal that collaboration in decentralized settings permits the use of larger learning rates. Zhu et al. [109] first explicitly characterize the implicit bias of decentralized SGD by establishing its connection with random sharpness-aware

minimization, proving the existence of flatne bias in decentralized training. Complementing this, Cao et al. [7] offer a detailed analysis of the interplay between flatness and optimization in DSGD, particularly its ability to escape local minima. More recently, Wu and Sun [93] investigate the implicit regularization properties of decentralized optimization in non-convex sparse regression problems, recovering the convergence rates achieved by gradient descent in centralized settings.

**Comparison with Zhu et al. [109].** We note that Zhu et al. [109] has highlighted the generalization benefits of decentralized learning, but key differences exist in terms of the experimental setup and the insights derived. While Zhu et al. [109] focuses on IID scenarios and specific cases involving exceptionally large batch sizes, we consider the more realistic non-IID setting using standard batch sizes. This shift in focus allows us to uncover phenomena not observed by Zhu et al. [109], including insights into communication allocation strategies and the surge-and-decline pattern.

## C Additional Experiments

### C.1 Experimental Setups

**Computational Resources.** The experiments were conducted on a computing facility equipped with 80 GB NVIDIA<sup>®</sup> A100<sup>™</sup> GPUs. All implementations are based on PyTorch, and computations are distributed across multiple GPUs for efficiency.

**Dataset.** We use three widely adopted image classification datasets: CIFAR-10, CIFAR-100 [45], and Tiny ImageNet [46]. CIFAR-10 consists of 60,000 RGB images across 10 classes, while CIFAR-100 contains 60,000 RGB images across 100 classes. The images in both datasets have a spatial resolution of  $32 \times 32$  pixels. Tiny ImageNet is a subset of the ImageNet dataset, comprising 100,000 images drawn from 200 classes, with each image resized to  $64 \times 64$  pixels. It provides a mid-scale benchmark that is more challenging than CIFAR datasets but less computationally demanding than training full ImageNet. To incorporate data augmentation, we employ a combination of RandomCrop with 4-pixel padding, RandomHorizontalFlip, and RandAugment with num\_ops=2 and magnitude=9.

**Details of Decentralized Learning.** We simulate a heterogeneous decentralized learning environment with  $m = 16$  agents, employing a Dirichlet distribution characterized by  $\alpha = 0.1$ . The Dirichlet distribution is commonly used to partition data in federated learning scenarios, as it allows for the control of label distribution skew among agents [103, 35]. A smaller  $\alpha$  results in more imbalanced data distributions, where some agents predominantly receive data from a limited number of classes, while a larger  $\alpha$  results in more uniform label distributions across agents. This configuration effectively captures the realistic non-IID nature of decentralized learning, where different agents may have access to personalized data reflective of their local environments.

- **Communication Graph.** We evaluate three decentralized communication topologies: random graph, ring graph, and exponential graph. In the random graph setting, during each communication round, each agent selects a random subset of its neighbors for gossip averaging. For "R 1", each agent selects exactly one random neighbor in each round. For "R 0.2", each agent selects one neighbor with a probability of 0.2 and continues local training without communication with a probability of 0.8. The ring graph enforces a fixed cyclic communication structure, while the exponential graph ensures connectivity by allowing agents to communicate with exponentially increasing distances in the ring graph.
- **Communication Rounds and Local Steps.** The decentralized learning process is conducted over  $T = 300$  communication rounds. We use a local training step size of  $H = 100$  batches per communication round to balance communication and computation costs.
- **Local Data per Agent.** Each agent is assigned a subset of the dataset with a fixed size of 4096 samples, drawn according to a Dirichlet distribution to simulate realistic non-IID scenarios. Due to the limited dataset size in CIFAR-10 and CIFAR-100, assigning fixed-size subsets can lead to overlapping samples among agents, particularly when  $\alpha$  is small.

**Model Architecture.** To ensure a representative comparison across different model families, we adopt ResNet-18 [33] and CLIP ViT-B/32 [69] as backbone architectures in our experiments. ResNet-18 is a widely used lightweight convolutional neural network that serves as a canonical example of traditional CNN-based architectures. In contrast, CLIP ViT-B/32 is a transformer-based vision model pre-trained on large-scale image-text pairs. For experiments on Tiny ImageNet, where images are

resized to 64×64 pixels, we adjust the CLIP visual encoder to handle the lower resolution. With a patch size of 32, each image yields 4 visual tokens arranged in a 2×2 grid, plus a [CLS] token, resulting in a 5-token input sequence.

**Implementation Details.** The training process is optimized using decentralized AdamW, as it has been shown to handle heterogeneous data distributions effectively. All hyperparameters are tuned through grid search based on global generalization performance. For ResNet-18 on CIFAR-100 and Tiny ImageNet, we use a learning rate of  $5 \times 10^{-4}$  when training from scratch, and  $1 \times 10^{-3}$  when fine-tuning from ImageNet-pretrained weights. For training CLIP pretrained ViT-B/32 on Tiny ImageNet, the learning rate is set to  $1 \times 10^{-5}$ . Weight decay is set to  $5 \times 10^{-4}$ , and the batch size is fixed at 128 for all experiments. To validate the consistency of our empirical observations, we conduct additional experiments using decentralized SGD and perform a systematic sensitivity analysis over a broad range of learning rates and batch sizes. The key empirical results remain consistent across these variations, indicating that our conclusions are stable and not sensitive to specific hyperparameter configurations.

**Computational Resource Requirements and Runtime.** To enhance accessibility for researchers working with diverse computational environments, our code includes a centralized simulation of decentralized training. This enables the reproduction and extension of our decentralized learning experiments using fewer GPUs. A single decentralized AdamW training experiment with 16 agents using ResNet-18 on the Tiny ImageNet dataset requires approximately 15 GB of GPU memory and can be conducted on a single GPU with sufficient memory, such as an NVIDIA V100, RTX 3090, RTX 4090, or A100. On an A100 GPU, the typical runtime is approximately 8 hours for 300 communication rounds, each comprising 100 local steps. For the CLIP ViT-B/32 model, the memory demand rises to about 30 GB, yet it remains feasible on a single A100 GPU, with a runtime of approximately 12 hours under the same configuration of 300 communication rounds and 100 local steps per round.

**Limitations.** Our empirical findings primarily focus on tasks within the vision domain. Although this is consistent with most existing decentralized learning literature [55, 43, 99, 86, 51, 104], extending the experimental setup to broader tasks is a meaningful direction for future research.

## C.2 Additional Experiments

We experiments with different initialization schemes, communication topologies, and optimizers to examine whether the empirical observations remain consistent.

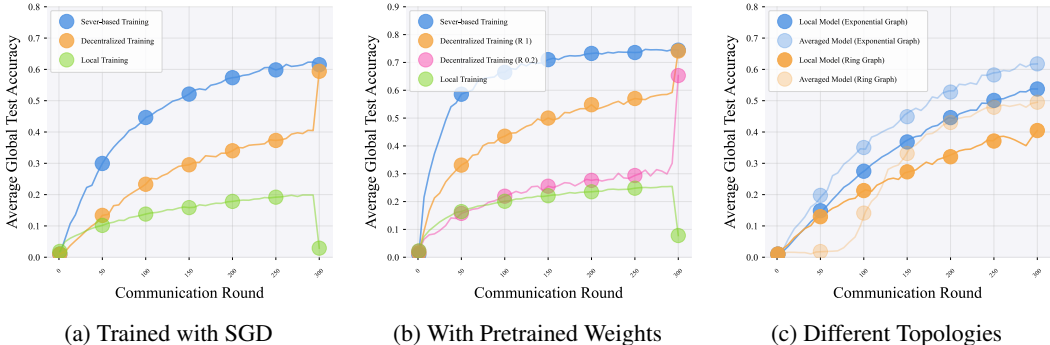


Figure C.1: Comparisons of global test accuracy (see Definition 2) in training of ResNet-18 on the Tiny ImageNet, distributed across 16 agents with high heterogeneity (Dirichlet  $\alpha = 0.1$ ; see details in Appendix C.1). We evaluate the effects of (a) different optimizers, (b) initialization schemes, and (c) communication topologies, under a highly heterogeneous data partition (Dirichlet  $\alpha = 0.1$ ) across 16 agents. Pretrained weights are used only in the second setting.

- **Model remains mergeable under even lower communication with pretraining.** With pretraining, the increase in test accuracy after single merging becomes more pronounced under lower communication (i.e., each agent communicates with one random peer at each round with probability 0.2; see Figure C.1b). However, local training alone still fails to guarantee global merging. The large

gap between the orange and green curves further supports our conclusion in [Subsection 4.3](#) that mergeability stems from limited yet nonzero communication rather than from pretraining itself.

- **Model remains mergeable across different communication topologies.** We evaluate two topologies: exponential and ring graphs. As shown in [Figure C.1c](#), both topologies preserve the mergeability of local models, with exponential graphs yielding slightly better generalization for both local and merged models. This suggests that the overall trend of mergeability persists across topologies, though performance may vary.

- **Model remains mergeable across different optimizers.** We also test whether the findings generalize from AdamW to SGD. As shown in [Figure C.1a](#), even with SGD, a single global merging at the end still significantly improves global test accuracy. In contrast, local training followed by merging again leads to degraded generalization, consistent with earlier results.

We further experiments with different hyperparameters (e.g., learning rate and batch size), dataset, and degree of data heterogeneity to examine whether the empirical observations remain consistent.

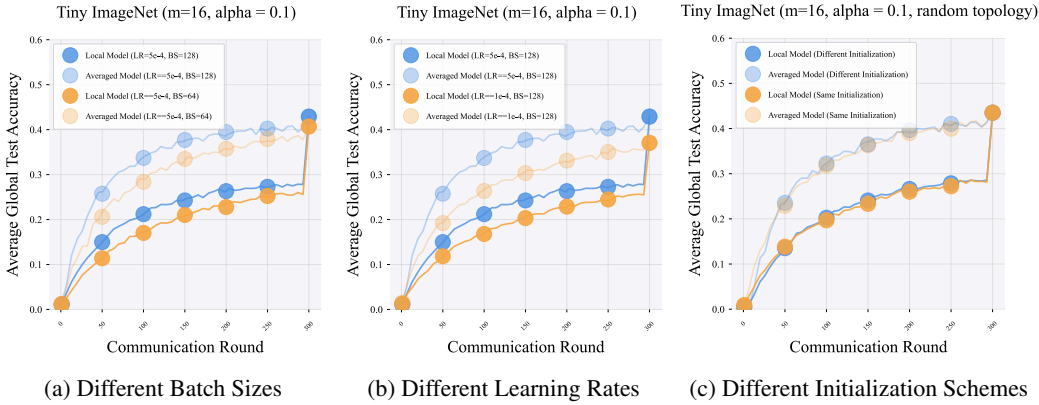


Figure C.2: Comparisons of global test accuracy (see [Definition 2](#)) in training of ResNet-18 on the Tiny ImageNet, distributed across 16 agents with high heterogeneity (Dirichlet  $\alpha = 0.1$ ; see details in [Appendix C.1](#)). We evaluate the effects of different (a) batch sizes (64 vs. 128), (b) learning rates ( $5 \times 10^{-4}$  vs.  $1 \times 10^{-4}$ ), and (c) different initialization schemes.

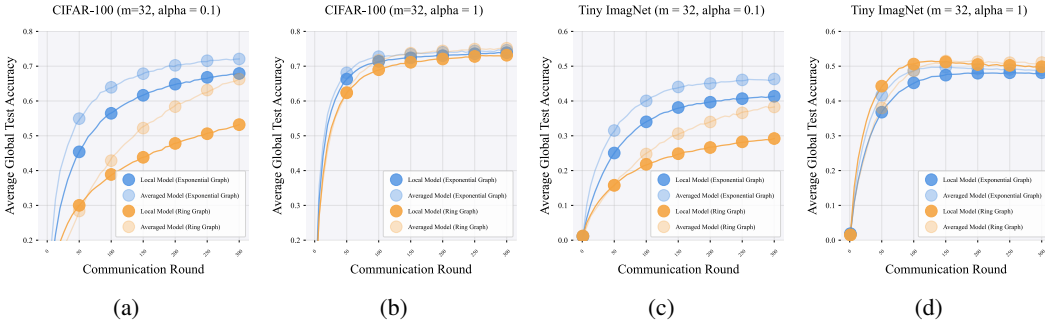


Figure C.3: Comparison of global test accuracy (see [Definition 2](#)) for ResNet-18 trained with 32 agents under different levels of data heterogeneity (Dirichlet  $\alpha = 0.1$  (a, c) vs.  $\alpha = 1.0$  (b, d); see [Appendix C.1](#)). Results are shown on both CIFAR-100 (a, b) and Tiny ImageNet (c, d).

**Summary.** Consistent results across a wide range of settings are observed, including different hyperparameter setups, datasets, degree of data heterogeneity, model architectures, optimizers, initialization schemes, and communication topologies.

## D Theory

This section provides the proofs of the main theoretical results presented in this paper. For simplicity, and following the setup in the existing literature, we assume that the sample size of local agents is  $n_k = n$  for all  $k \in \mathcal{V}$ .

**Lemma D.1** (Consensus Distance Recursion under Local Updates [43]). *Suppose **Assumption 1–Assumption 3** hold. Let  $\theta_k^{(t)}$  be the local parameter on client  $k$  at  $t$ -th step, and denote their average by  $\bar{\theta}^{(t)} = \frac{1}{m} \sum_{k=1}^m \theta_k^{(t)}$ . Define the consensus distance and the average gradient norm at round  $t$  by  $\Xi_t^2 = \frac{1}{m} \sum_{k=1}^m \|\theta_k^{(t)} - \bar{\theta}^{(t)}\|^2$  and  $\phi_t^2 = \frac{1}{m} \sum_{k=1}^m \|\nabla \mathcal{L}_k(\theta_k^{(t)})\|^2$ , where  $\mathcal{L}_k(\theta) = \mathbb{E}_{\xi_k \sim \mathcal{D}_k}[\mathcal{L}(\theta; \xi_k)]$ . Let  $\eta > 0$  the learning rate, and  $\sigma^2$  the variance bound from **Assumption 3**. Then there exists a constant  $p > 0$  (see **Assumption 1**) such that for all  $t \geq 0$ , the following inequality holds:*

$$\mathbb{E} [\Xi_{t+1}^2] \leq \left(1 - \frac{p}{2}\right) \Xi_t^2 + \frac{6(1-p)}{p} \eta^2 (\phi_t^2 + \sigma^2), \quad (\text{D.1})$$

where the expectation is taken over the stochastic gradients in the  $t$ -th update phase.

*Proof.* For completeness, we provide the proof of **Lemma D.1**, with minor corrections and additional details. In decentralized SGD (**Algorithm 1** with SGD as the local optimizer), each agent  $k \in \mathcal{V}$  performs at each iteration

$$\theta_k^{(t+1)} = \sum_{l=1}^m W_{k,l} (\theta_l^{(t)} - \eta \nabla \mathcal{L}_k(\theta_l^{(t)}; \xi_l^{(t)})).$$

In matrix form, letting

$$\Theta^{(t)} = [\theta_1^{(t)}, \dots, \theta_m^{(t)}] \in \mathbb{R}^{d \times m}, \quad \nabla \mathcal{L}(\Theta^{(t)}; \xi^{(t)}) = [\nabla \mathcal{L}_1(\theta_1^{(t)}; \xi_1^{(t)}), \dots, \nabla \mathcal{L}_m(\theta_m^{(t)}; \xi_m^{(t)})],$$

we have

$$\Theta^{(t+1)} = (\Theta^{(t)} - \eta \nabla \mathcal{L}(\Theta^{(t)}; \xi^{(t)})) W.$$

The consensus matrix after mixing is

$$\bar{\Theta}^{(t+1)} = \Theta^{(t+1)} \frac{1}{m} \mathbf{1} \mathbf{1}^\top = (\Theta^{(t)} - \eta \nabla \mathcal{L}(\Theta^{(t)}; \xi^{(t)})) \frac{1}{m} \mathbf{1} \mathbf{1}^\top,$$

since  $\mathbf{1}^\top W = \mathbf{1}^\top$ .

Thus the consensus distance satisfies

$$m \Xi_{t+1}^2 = \|\Theta^{(t+1)} - \bar{\Theta}^{(t+1)}\|_F^2 = \|(\Theta^{(t)} - \eta \nabla \mathcal{L}(\Theta^{(t)}; \xi^{(t)})) (W - \frac{1}{m} \mathbf{1} \mathbf{1}^\top)\|_F^2.$$

By **Assumption 1**, for any  $\Theta \in \mathbb{R}^{d \times m}$ ,

$$\mathbb{E}_W \|\Theta W - \bar{\Theta}\|_F^2 \leq (1 - \rho) \|\Theta - \bar{\Theta}\|_F^2,$$

we obtain,

$$m \Xi_{t+1}^2 \leq (1 - p) \left\| \Theta^{(t)} \left( I - \frac{1}{m} \mathbf{1} \mathbf{1}^\top \right) - \eta \nabla \mathcal{L}(\Theta^{(t)}; \xi^{(t)}) \left( I - \frac{1}{m} \mathbf{1} \mathbf{1}^\top \right) \right\|_F^2.$$

Applying the inequality  $\|A + B\|_F^2 \leq (1 + \alpha) \|A\|_F^2 + (1 + 1/\alpha) \|B\|_F^2$  with  $\alpha = \frac{p}{2}$  gives

$$\begin{aligned} m \Xi_{t+1}^2 &\leq (1 - p) \left[ \left(1 + \frac{p}{2}\right) \left\| \Theta^{(t)} \left( I - \frac{1}{m} \mathbf{1} \mathbf{1}^\top \right) \right\|_F^2 + \left(1 + \frac{2}{p}\right) \eta^2 \left\| \nabla \mathcal{L}(\Theta^{(t)}; \xi^{(t)}) \right\|_F^2 \right] \\ &\leq \left(1 - \frac{p}{2}\right) m \Xi_t^2 + \frac{6(1-p)}{p} \eta^2 \left\| \nabla \mathcal{L}(\Theta^{(t)}; \xi^{(t)}) \right\|_F^2, \end{aligned}$$

where we used  $(1 + p/2) \leq 1 + p$  and  $(1 + 2/p) \leq 6/p$  for  $p \in (0, 1)$ .

We now decompose the stochastic gradient as

$$\nabla \mathcal{L}(\Theta^{(t)}; \xi^{(t)}) = \nabla \mathcal{L}(\Theta^{(t)}) + [\nabla \mathcal{L}(\Theta^{(t)}; \xi^{(t)}) - \nabla \mathcal{L}(\Theta^{(t)})],$$

so

$$\|\nabla\mathcal{L}(\Theta^{(t)}; \xi^{(t)})\|_F^2 \leq 2\|\nabla\mathcal{L}(\Theta^{(t)})\|_F^2 + 2\|\nabla\mathcal{L}(\Theta^{(t)}; \xi^{(t)}) - \nabla\mathcal{L}(\Theta^{(t)})\|_F^2.$$

Taking expectation over  $\xi^{(t)}$  and invoking [Assumption 3](#), we get

$$\mathbb{E}[\|\nabla\mathcal{L}(\Theta^{(t)}; \xi^{(t)})\|_F^2] \leq 2\|\nabla\mathcal{L}(\Theta^{(t)})\|_F^2 + 2\sigma^2 m.$$

Substituting back and dividing by  $m$  yields

$$\mathbb{E}[\Xi_{t+1}^2] \leq \left(1 - \frac{p}{2}\right) \Xi_t^2 + \frac{6(1-p)}{p} \eta^2 (\phi_t^2 + \sigma^2),$$

which completes the proof.  $\square$

**Corollary D.2** ([43]). *Define the consensus distance and the average gradient norm at round  $t$  by  $\Xi_t^2 = \frac{1}{m} \sum_{k=1}^m \|\theta_k^{(t)} - \bar{\theta}^{(t)}\|^2$  and  $\phi_t^2 = \frac{1}{m} \sum_{k=1}^m \|\nabla\mathcal{L}_k(\theta_k^{(t)})\|^2$ , where  $\mathcal{L}_k(\theta) = \mathbb{E}_{\xi_k \sim \mathcal{D}_k} [\mathcal{L}(\theta; \xi_k)]$ . Under the conditions of [Lemma D.1](#), suppose that for all iterations  $t$ , the gradient norms are uniformly bounded by a constant  $\phi$ , i.e.  $\phi_t \leq \phi, \forall t \in \{1, \dots, T\}$ . Then the expected consensus distance satisfies*

$$\mathbb{E}[\Xi_t^2] \leq 12(1-p) \eta^2 \left( \frac{\phi^2}{p^2} + \frac{\sigma^2}{p} \right).$$

*In the general case where the gradient-norms change slowly, i.e.,  $\phi_t^2 \leq (1 + \frac{p}{4}) \phi_{t+1}^2$ , we have*

$$\mathbb{E}[\Xi_t^2] \leq 24(1-p) \eta^2 \left( \frac{\phi_{t-1}^2}{p^2} + \frac{\sigma^2}{p} \right).$$

*The expectation here is taken over the stochastic gradients in the  $t$ -th update phase.*

*Proof.* Consider the key recursion from [Lemma D.1](#):

$$\mathbb{E}[\Xi_{t+1}^2] \leq \left(1 - \frac{p}{2}\right) \Xi_t^2 + \frac{6(1-p)}{p} \eta^2 (\phi_t^2 + \sigma^2).$$

**(1) Special Case: uniformly bounded gradient norms.**

Assume  $\phi_t \leq \phi$ . Unrolling the above gives

$$\mathbb{E}[\Xi_{t+1}^2] \leq \sum_{i=0}^{t-1} \left(1 - \frac{p}{2}\right)^i \frac{6(1-p)}{p} \eta^2 (\phi^2 + \sigma^2).$$

Since  $\sum_{i=0}^{t-1} \left(1 - \frac{p}{2}\right)^i \leq \frac{2}{p}$ , we can bound the consensus distance as

$$\mathbb{E}[\Xi_{t+1}^2] \leq \frac{6(1-p)}{p} \eta^2 (\phi^2 + \sigma^2) \times \frac{2}{p} = \frac{12(1-p) \eta^2}{p^2} (\phi^2 + \sigma^2),$$

which yields the first claim.

**(2) General Case: slowly changing gradient norms.**

If  $\phi_t^2 \leq (1 + \frac{p}{4}) \phi_{t+1}^2$ , then

$$\left(1 - \frac{p}{2}\right)^i \left(1 + \frac{p}{4}\right)^i \leq \left(1 - \frac{p}{4}\right)^i.$$

Thus, the consensus distance satisfies

$$\begin{aligned} \mathbb{E}[\Xi_{t+1}^2] &\leq \sum_{i=0}^{t-i-1} \left(1 - \frac{p}{2}\right)^i \frac{6(1-p) \eta^2 (\phi_{t-i-1}^2 + p\sigma^2)}{p} \\ &\leq \sum_{i=0}^{t-1} \left(1 - \frac{p}{4}\right)^i \frac{6(1-p) \eta^2 (\phi_{t-i-1}^2 + p\sigma^2)}{p} \leq \frac{24(1-p) \eta^2}{p^2} (\phi_{t-1}^2 + \sigma^2). \end{aligned} \quad (\text{D.2})$$

$\square$

**Proposition D.3** (Implicit Bias of Decentralized SGD [109]). Assume  $\mathcal{L} \in C^4(\mathbb{R}^d)$ , the globally averaged model of decentralized SGD (DSGD), defined by  $\bar{\theta}^{(t)} = \frac{1}{m} \sum_{k=1}^m \theta_k^{(t)}$ , follows the following gradient descent direction:

$$\mathbb{E}_{\xi^{(t)}}[\bar{\theta}^{(t+1)}] = \bar{\theta}^{(t)} - \eta \cdot \mathbb{E}_{\epsilon^{(t)} \sim \mathcal{N}(0, \Gamma^{(t)})} \left[ \nabla \mathcal{L}(\bar{\theta}^{(t)} + \epsilon^{(t)}) \right] + \delta^{(t)},$$

where  $\Gamma^{(t)} = \frac{1}{m} \sum_{k=1}^m (\theta_k^{(t)} - \bar{\theta}^{(t)})(\theta_k^{(t)} - \bar{\theta}^{(t)})^\top \in \mathbb{R}^{m \times m}$  denotes the consensus distance matrix, and  $\delta^{(t)} = \Theta \left( \frac{\eta}{m} \sum_{k=1}^m \|\theta_k^{(t)} - \bar{\theta}^{(t)}\|_2^3 \right)$  denotes the high-order terms. The first expectation eliminates the randomness from sampled data  $\xi^{(t)} = \{\xi_k^{(t)}\}_{k \in \mathcal{V}}$  at step  $(t)$ .

We can then control the expected squared distance between two consecutive steps of the globally averaged model with [Corollary D.4](#).

**Corollary D.4.** Under the assumptions in [Proposition D.3](#), the expected squared distance between two consecutive iterates of decentralized SGD can be bounded as follows:

$$\mathbb{E}_{\xi^{(t)}} \|\bar{\theta}^{(t+1)} - \bar{\theta}^{(t)}\|^2 \leq \frac{\sigma^2}{m} + \eta^2 \left\| \nabla \mathcal{L}(\bar{\theta}^{(t)}) + \nabla \text{Tr}(\nabla^2 \mathcal{L}(\bar{\theta}^{(t)}) \Gamma^{(t)}) + \delta^{(t)} \right\|^2. \quad (\text{D.3})$$

*Proof.* Denote  $\gamma^{(t+1)} = \mathbb{E}_{\xi^{(t)}} \bar{\theta}^{(t+1)} - \bar{\theta}^{(t)}$ . We can expand the expected distance as follows:

$$\begin{aligned} \mathbb{E}_{\xi^{(t)}} \|\bar{\theta}^{(t+1)} - \bar{\theta}^{(t)}\|^2 &= \mathbb{E}_{\xi^{(t)}} \|\bar{\theta}^{(t+1)}\|^2 - \|\bar{\theta}^{(t)}\|^2 - 2(\bar{\theta}^{(t)})^\top \gamma^{(t+1)} \\ &= \text{Tr}(\text{Cov}(\bar{\theta}^{(t+1)})) + \|\mathbb{E}_{\xi^{(t)}} \bar{\theta}^{(t+1)}\|^2 - \|\bar{\theta}^{(t)}\|^2 - 2(\bar{\theta}^{(t)})^\top \gamma^{(t+1)} \\ &= \text{Tr}(\text{Cov}(\bar{\theta}^{(t+1)})) + \|\mathbb{E}_{\xi^{(t)}} [\bar{\theta}^{(t+1)} - \bar{\theta}^{(t)}]\|^2 \\ &= \text{Tr} \left( \text{Cov} \left( \frac{1}{m} \sum_{k=1}^m \nabla \mathcal{L}(\theta_k^{(t)}; \xi_k^{(t)}) \right) \right) + \|\mathbb{E}_{\xi^{(t)}} [\bar{\theta}^{(t+1)} - \bar{\theta}^{(t)}]\|^2, \end{aligned} \quad (\text{D.4})$$

where in the second equality we substitute  $\mathbb{E}_{\xi^{(t)}} \bar{\theta}^{(t+1)}$  with  $\gamma^{(t+1)} + \bar{\theta}^{(t)}$ . The final equality is derived from the update rule:

$$\bar{\theta}^{(t+1)} = \bar{\theta}^{(t)} - \frac{1}{m} \sum_{k=1}^m \nabla \mathcal{L}(\theta_k^{(t)}; \xi_k^{(t)}).$$

According to the convexity of the vector norm and the fact that

$$\text{Tr} \left( \text{Cov} \left( \frac{1}{m} \sum_{k=1}^m \nabla \mathcal{L}(\theta_k^{(t)}; \xi_k^{(t)}) \right) \right) = \mathbb{E}_{\xi^{(t)}} \left\| \frac{1}{m} \sum_{k=1}^m \nabla \mathcal{L}(\theta_k^{(t)}; \xi_k^{(t)}) - \frac{1}{m} \sum_{k=1}^m \mathbb{E}_{\xi_k^{(t)}} \nabla \mathcal{L}(\theta_k^{(t)}; \xi_k^{(t)}) \right\|^2, \quad (\text{D.5})$$

we then complete the proof by applying [Proposition D.3](#) and the bounded noise assumption in [Assumption 3](#).  $\square$

**Corollary D.5.** Let  $\Gamma^{(t)} = \frac{1}{m} \sum_{k=1}^m (\theta_k^{(t)} - \bar{\theta}^{(t)})(\theta_k^{(t)} - \bar{\theta}^{(t)})^\top \in \mathbb{R}^{d \times d}$ , where  $\bar{\theta}^{(t)} = \frac{1}{m} \sum_{k=1}^m \theta_k^{(t)} \in \mathbb{R}^d$  denotes the globally averaged model across  $m$  agents. Assume the loss function  $\mathcal{L} \in C^4(\mathbb{R}^d)$ , with its fourth derivative  $\nabla^4 \mathcal{L}(\cdot)$  uniformly bounded by a constant  $L_4 > 0$ , i.e.,  $\|\nabla^4 \mathcal{L}(\cdot)\| \leq L_4$ . Then, for  $\epsilon^{(t)} \sim \mathcal{N}(0, \Gamma^{(t)})$ , the expected gradient perturbation satisfies:

$$\begin{aligned} \mathbb{E}_{\epsilon^{(t)} \sim \mathcal{N}(0, \Gamma^{(t)})} \left[ \nabla \mathcal{L}(\bar{\theta}^{(t)} + \epsilon^{(t)}) \right] - \nabla \mathcal{L}(\bar{\theta}^{(t)}) \\ = \nabla \text{Tr} \left( \nabla^2 \mathcal{L}(\bar{\theta}^{(t)}) \Gamma^{(t)} \right) + \mathbb{E}_{\epsilon^{(t)} \sim \mathcal{N}(0, \Gamma^{(t)})} \left[ R_3(\epsilon^{(t)}) \right], \end{aligned} \quad (\text{D.6})$$

where  $\|R_3(\epsilon^{(t)})\|$  is bounded by  $\frac{L_4}{24} \|\epsilon^{(t)}\|^3$ .

*Proof.* We apply the third-order Taylor expansion to  $\nabla\mathcal{L}$  around  $\bar{\theta}^{(t)}$ :

$$\nabla\mathcal{L}(\bar{\theta}^{(t)} + \epsilon^{(t)}) = \nabla\mathcal{L}(\bar{\theta}^{(t)}) + \nabla^2\mathcal{L}(\bar{\theta}^{(t)})\epsilon^{(t)} + \frac{1}{2}\nabla^3\mathcal{L}(\bar{\theta}^{(t)})[\epsilon^{(t)}, \epsilon^{(t)}] + R_3(\epsilon^{(t)}),$$

with the remainder:

$$R_3(\epsilon^{(t)}) = \int_0^1 \frac{(1-\tau)^3}{6} \nabla^4\mathcal{L}(\bar{\theta}^{(t)} + \tau\epsilon^{(t)})[\epsilon^{(t)}, \epsilon^{(t)}, \epsilon^{(t)}] d\tau.$$

Taking expectations over  $\epsilon^{(t)} \sim \mathcal{N}(0, \Gamma^{(t)})$ , since  $\mathbb{E}[\epsilon^{(t)}] = 0$ , the linear term vanishes. The quadratic term  $\mathbb{E}[\nabla^3\mathcal{L}(\bar{\theta}^{(t)})[\epsilon^{(t)}, \epsilon^{(t)}]]$  simplifies to  $\nabla \text{Tr}(\nabla^2\mathcal{L}(\bar{\theta}^{(t)})\Gamma^{(t)})$  due to properties of the Gaussian distribution. The remainder bound can be bounded as

$$\|R_3(\epsilon^{(t)})\| \leq \int_0^1 \frac{(1-\tau)^3}{6} L_4 \|\epsilon^{(t)}\|^3 d\tau = L_4 \|\epsilon^{(t)}\|^3 \cdot \frac{1}{6} \int_0^1 (1-\tau)^3 d\tau.$$

Since  $\int_0^1 (1-\tau)^3 d\tau = \frac{1}{4}$ , we have:

$$\|R_3(\epsilon^{(t)})\| \leq L_4 \|\epsilon^{(t)}\|^3 \cdot \frac{1}{6} \cdot \frac{1}{4} = \frac{L_4}{24} \|\epsilon^{(t)}\|^3.$$

□

For comparison, we restate the convergence rate of DSGD by Koloskova et al. [42].

**Theorem D.6** (Non-convex Convergence Rate of DSGD [42]). *Under Assumption 1, Assumption 2 and Assumption 3, let the learning rate  $\eta$  satisfy  $\eta \leq \eta_{\max} = \mathcal{O}(\frac{\rho}{L})$  let  $\bar{\theta}^{(t)} = \frac{1}{m} \sum_{k=1}^m \theta_k^{(t)}$  denote the averaged model at the  $t$ -th step. Then there exists an optimal learning rate  $\eta \leq \eta_{\max}$  such that*

$$\frac{1}{T} \sum_{t=0}^{T-1} \mathbb{E} \left[ \|\nabla\mathcal{L}(\bar{\theta}^{(t)})\|_2^2 \right] \leq \varepsilon,$$

after total number of steps

$$T = \mathcal{O} \left( \frac{\sigma^2}{m\varepsilon^2} + \frac{\sqrt{p}\sigma + \zeta}{p\varepsilon^{3/2}} + \frac{1}{p\varepsilon} \right) \cdot L(\mathcal{L}(\theta_0) - \mathcal{L}^*).$$

We then provide our main theoretical results as follows.

**Theorem D.7** (Non-convex Convergence Rate of DSGD). *Suppose Assumption 2 and Assumption 3 hold. Consider decentralized SGD (DSGD) with learning rate satisfying  $\eta \leq \frac{1}{L}$ , and let  $\bar{\theta}^{(t)} = \frac{1}{m} \sum_{k=1}^m \theta_k^{(t)}$  denote the averaged model at the  $t$ -th step. It holds that  $\frac{1}{T} \sum_{t=0}^{T-1} \mathbb{E} \left[ \|\nabla\mathcal{L}(\bar{\theta}^{(t)})\|_2^2 \right] \leq \varepsilon$ , after total number of steps*

$$T = \mathcal{O} \left( \frac{\sigma^2}{m\varepsilon^2} + \frac{1}{\varepsilon} + \frac{1}{\varepsilon^2} \sum_t A^{(t)} \right) \cdot L(\mathcal{L}(\theta^{(0)}) - \mathcal{L}^*),$$

where  $A^{(t)} \triangleq \eta L (2T_2 + L_3^2 \Xi_t^4 + (2L_1 + 2L_3 \Xi_t^2 + \frac{mL_4^2}{24^2}) \sqrt{m} \Xi_t^3)$ . Here,  $T_2 = (\nabla^2\mathcal{L}(\bar{\theta}^{(t)})\Gamma^{(t)})^\top \nabla \text{Tr}(\nabla^2\mathcal{L}(\bar{\theta}^{(t)})\Gamma^{(t)})$ , and  $\Xi_t^2 = \text{Tr}(\Gamma^{(t)})$  with  $\Gamma^{(t)} = \frac{1}{m} \sum_{k=1}^m (\theta_k^{(t)} - \bar{\theta}^{(t)})(\theta_k^{(t)} - \bar{\theta}^{(t)})^\top$ . Constants  $L_1, L_3, L_4$  satisfy  $\|\nabla^q\mathcal{L}(\theta)\| \leq L_q$  for  $q = 1, 3, 4, \forall \theta$ .

*Proof.* We structure the proof into several key steps.

#### Step (A): Descent Force Decomposition.

Based on the  $L$ -smoothness of the loss function  $\mathcal{L}$  (refer to Assumption 2), we can apply the first-order Taylor expansion around  $\bar{\theta}^{(t)}$  to establish an upper bound for  $\mathcal{L}(\bar{\theta}^{(t+1)})$ :

$$\mathcal{L}(\bar{\theta}^{(t+1)}) \leq \mathcal{L}(\bar{\theta}^{(t)}) + \nabla\mathcal{L}(\bar{\theta}^{(t)})^\top (\bar{\theta}^{(t+1)} - \bar{\theta}^{(t)}) + \frac{L}{2} \|\bar{\theta}^{(t+1)} - \bar{\theta}^{(t)}\|^2.$$

According to [Proposition D.3](#), we have

$$\mathbb{E}_{\xi^{(t)}}[\bar{\theta}^{(t+1)}] = \bar{\theta}^{(t)} - \eta (\nabla \mathcal{L}(\bar{\theta}^{(t)}) + \nabla \text{Tr}(\nabla^2 \mathcal{L}(\bar{\theta}^{(t)})\Gamma^{(t)})) + \delta^{(t)},$$

where  $\bar{\theta}^{(t+\frac{1}{2})} = \bar{\theta}^{(t)} + \epsilon^{(t)}$  and  $\epsilon^{(t)} \sim \mathcal{N}(0, \Gamma^{(t)})$ .

Substituting this into the previous bound and taking the expectation with respect to random data sampling yields:

$$\begin{aligned} & \mathbb{E}_{\xi^{(t)}}[\mathcal{L}(\bar{\theta}^{(t+1)})] \\ & \leq \mathcal{L}(\bar{\theta}^{(t)}) - \eta \nabla \mathcal{L}(\bar{\theta}^{(t)})^\top \left( \nabla \mathcal{L}(\bar{\theta}^{(t)}) + \nabla \text{Tr}(\nabla^2 \mathcal{L}(\bar{\theta}^{(t)})\Gamma^{(t)}) - \delta^{(t)} \right) + \mathbb{E}_{\xi^{(t)}} \frac{\eta^2 L}{2} \|\bar{\theta}^{(t+1)} - \bar{\theta}^{(t)}\|^2. \end{aligned}$$

According to [Corollary D.4](#), we obtain

$$\mathbb{E}_{\xi^{(t)}} \|\bar{\theta}^{(t+1)} - \bar{\theta}^{(t)}\|^2 \leq \frac{\sigma^2}{m} + \eta^2 \|\nabla \mathcal{L}(\bar{\theta}^{(t)}) + \nabla \text{Tr}(\nabla^2 \mathcal{L}(\bar{\theta}^{(t)})\Gamma^{(t)}) + \delta^{(t)}\|^2.$$

To further refine the analysis, we decompose the squared norm:

$$\begin{aligned} & \|\nabla \mathcal{L}(\bar{\theta}^{(t)}) + \nabla \text{Tr}(\nabla^2 \mathcal{L}(\bar{\theta}^{(t)})\Gamma^{(t)})\|^2 \\ & = \|\nabla \text{Tr}(\nabla^2 \mathcal{L}(\bar{\theta}^{(t)})\Gamma^{(t)})\|^2 + \|\nabla \mathcal{L}(\bar{\theta}^{(t)})\|^2 + 2 \nabla \text{Tr}(\nabla^2 \mathcal{L}(\bar{\theta}^{(t)})\Gamma^{(t)})^\top \nabla \mathcal{L}(\bar{\theta}^{(t)}). \end{aligned}$$

Combining the previous steps, we obtain:

$$\begin{aligned} \mathbb{E}_{\xi^{(t)}} \mathcal{L}(\bar{\theta}^{(t+1)}) & \leq \mathcal{L}(\bar{\theta}^{(t)}) - (\eta - \frac{\eta^2 L}{2}) \underbrace{\|\nabla \mathcal{L}(\bar{\theta}^{(t)})\|^2}_{T_2} + \frac{\eta^2 L}{2} \underbrace{\|\nabla \text{Tr}(\nabla^2 \mathcal{L}(\bar{\theta}^{(t)})\Gamma^{(t)})\|^2}_{T_1} \\ & \quad + \underbrace{\eta^2 L \nabla \mathcal{L}(\bar{\theta}^{(t)})^\top \nabla \text{Tr}(\nabla^2 \mathcal{L}(\bar{\theta}^{(t)})\Gamma^{(t)})}_{T_3} + \frac{\sigma^2}{m} \cdot \frac{\eta^2 L}{2} \\ & \quad + \underbrace{\eta^2 L (\nabla \mathcal{L}(\bar{\theta}^{(t)}) + \nabla \text{Tr}(\nabla^2 \mathcal{L}(\bar{\theta}^{(t)})\Gamma^{(t)}))^\top \delta^{(t)}}_{T_3} + \frac{\eta^2 L}{2} \underbrace{\|\delta^{(t)}\|^2}_{T_4}. \quad (\text{D.7}) \end{aligned}$$

We subsequently control terms related to  $\mathbb{E}_{\epsilon^{(t)} \sim \mathcal{N}(0, \Gamma^{(t)})} \nabla \mathcal{L}(\bar{\theta}^{(t+\frac{1}{2})}) - \nabla \mathcal{L}(\bar{\theta}^{(t)})$  in [Equation \(D.7\)](#).

### Step (B): Control Consensus-related Terms

Applying the logic in [Corollary D.5](#) to bound residuals, we can derive

$$\|\delta^{(t)}\| \leq \frac{L_4}{24} \cdot \frac{1}{m} \sum_{k=1}^m \|\theta_k^{(t)} - \bar{\theta}^{(t)}\|^3 \leq \frac{L_4}{24} \cdot \sqrt{m} \left( \frac{1}{m} \sum_{k=1}^m \|\theta_k^{(t)} - \bar{\theta}^{(t)}\|^2 \right)^{\frac{3}{2}},$$

and thus by the convexity of square operation,

$$T_4 = \|\delta^{(t)}\|^2 \leq \frac{m L_4^2}{24^2} \cdot \left( \frac{1}{m} \sum_{k=1}^m \|\theta_k^{(t)} - \bar{\theta}^{(t)}\|^2 \right)^3.$$

Given  $\|\nabla^3 \mathcal{L}(\cdot)\| \leq L_3$  we can upper-bound  $T_1$  as

$$T_1 = \|\nabla \text{Tr}(\nabla^2 \mathcal{L}(\bar{\theta}^{(t)})\Gamma^{(t)})\|^2 \leq L_3^2 \cdot \left( \frac{1}{m} \sum_{k=1}^m \|\theta_k^{(t)} - \bar{\theta}^{(t)}\|^2 \right)^2 = L_3^2 \cdot \left( \frac{1}{m} \sum_{k=1}^m \|\theta_k^{(t)} - \bar{\theta}^{(t)}\|^2 \right)^4.$$

We can also bound  $T_3$  as follows:

$$\begin{aligned} T_3 & \leq \|\nabla \text{Tr}(\nabla^2 \mathcal{L}(\bar{\theta}^{(t)})\Gamma^{(t)}) + \nabla \mathcal{L}(\bar{\theta}^{(t)})\| \cdot \frac{1}{m} \sum_{k=1}^m \|\theta_k^{(t)} - \bar{\theta}^{(t)}\|^3 \\ & \leq (L_3 \frac{1}{m} \sum_{k=1}^m \|\theta_k^{(t)} - \bar{\theta}^{(t)}\|^2 + L_1) \frac{1}{m} \sum_{k=1}^m \|\theta_k^{(t)} - \bar{\theta}^{(t)}\|^3 \end{aligned}$$

$$\leq (L_3 \frac{1}{m} \sum_{k=1}^m \|\theta_k^{(t)} - \bar{\theta}^{(t)}\|^2 + L_1) \sqrt{m} (\frac{1}{m} \sum_{k=1}^m \|\theta_k^{(t)} - \bar{\theta}^{(t)}\|^2)^{\frac{3}{2}}.$$

Recall the notation  $\Xi_t^2 = (\frac{1}{m} \sum_{k=1}^m \|\theta_k^{(t)} - \bar{\theta}^{(t)}\|^2)$ . Therefore,

$$A^{(t)} \triangleq \eta L (2T_2 + L_3^2 \Xi_t^4 + (2L_1 + 2L_3 \Xi_t^2 + \frac{mL_4^2}{24^2}) \sqrt{m} \Xi_t^3).$$

Then Equation (D.7) becomes

$$\mathbb{E}_{\xi^{(t)}} \mathcal{L}(\bar{\theta}^{(t+1)}) \leq \mathcal{L}(\bar{\theta}^{(t)}) - \left(\eta - \frac{\eta^2 L}{2}\right) \|\nabla \mathcal{L}(\bar{\theta}^{(t)})\|^2 + \eta^2 L A^{(t)} + \frac{\sigma^2}{m} \cdot \frac{\eta^2 L}{2}, \quad (\text{D.8})$$

where

$$A^{(t)} = \eta L (2T_2 + T_1 + 2T_3 + T_4) \leq 2T_2 + L_3^2 \Xi_t^4 + \left(2L_1 + 2L_3 \Xi_t^2 + \frac{mL_4^2}{24^2}\right) \sqrt{m} \Xi_t^3. \quad (\text{D.9})$$

### Step (C): Derive the Rate

Starting from the descent inequality (D.8):

$$\mathbb{E}_{\xi^{(t)}} [\mathcal{L}(\bar{\theta}^{(t+1)})] \leq \mathcal{L}(\bar{\theta}^{(t)}) - \left(\eta - \frac{\eta^2 L}{2}\right) \|\nabla \mathcal{L}(\bar{\theta}^{(t)})\|^2 + \eta^2 L A^{(t)} + \frac{\sigma^2}{m} \frac{\eta^2 L}{2}.$$

Taking full expectation and summing over  $t = 0, \dots, T-1$ , we obtain

$$\sum_{t=0}^{T-1} \left(\eta - \frac{\eta^2 L}{2}\right) \mathbb{E} \|\nabla \mathcal{L}(\bar{\theta}^{(t)})\|^2 \leq \mathcal{L}(\theta^{(0)}) - \mathbb{E} [\mathcal{L}(\bar{\theta}^{(T)})] + \eta^2 L \sum_{t=0}^{T-1} A^{(t)} + \frac{\sigma^2 \eta^2 L T}{2m}.$$

Since  $\eta \leq 1/L$  implies  $\eta - \frac{\eta^2 L}{2} \geq \eta/2$ , and denoting  $\Delta = \mathcal{L}(\theta^{(0)}) - \mathcal{L}^*$ , we get

$$\frac{1}{T} \sum_{t=0}^{T-1} \mathbb{E} \|\nabla \mathcal{L}(\bar{\theta}^{(t)})\|^2 \leq \frac{2\Delta}{\eta T} + \frac{2\eta L}{T} \sum_{t=0}^{T-1} A^{(t)} + \frac{\sigma^2 \eta L}{m}.$$

To ensure this is at most  $\varepsilon$ , it suffices to enforce

$$\frac{\sigma^2 \eta L}{m} + \frac{2\eta L}{T} \sum_{t=0}^{T-1} A^{(t)} \leq \frac{\varepsilon}{2}, \quad \frac{2\Delta}{\eta T} \leq \frac{\varepsilon}{2},$$

which suggest

$$\eta = \min \left\{ \frac{1}{L}, \frac{\varepsilon}{2} \cdot \frac{1}{\frac{\sigma^2 \eta L}{m} + \frac{2\eta L}{T} \sum_{t=0}^{T-1} A^{(t)}} \right\}, \quad \text{and} \quad T \geq \frac{4\Delta}{\eta \varepsilon}.$$

Therefore,

$$T = \mathcal{O} \left( \frac{L\Delta}{\varepsilon} + \frac{L\Delta\sigma^2}{m\varepsilon^2} + \frac{L\Delta}{\varepsilon^2} \sum_{t=0}^{T-1} A^{(t)} \right) = \mathcal{O} \left( \left( \frac{\sigma^2}{m\varepsilon^2} + \frac{1}{\varepsilon^2} \sum_{t=0}^{T-1} A^{(t)} + \frac{1}{\varepsilon} \right) L (\mathcal{L}(\theta^{(0)}) - \mathcal{L}^*) \right),$$

is sufficient to guarantee

$$\frac{1}{T} \sum_{t=0}^{T-1} \mathbb{E} \|\nabla \mathcal{L}(\bar{\theta}^{(t)})\|^2 \leq \varepsilon.$$

The proof is now complete.  $\square$

**Proposition D.8.** *Suppose Assumption 4 holds and assume that the gradient norm satisfies  $\|\nabla \mathcal{L}(\bar{\theta}^{(t)})\| \geq c_t > 0$  for positive constant  $c_t$ . Then, for any fixed  $m > 0$ , there exists a sufficiently small  $\Xi_t^2 > 0$ , where  $\Xi_t^2 = \text{Tr}(\Gamma^{(t)})$  with  $\Gamma^{(t)} = \frac{1}{m} \sum_{k=1}^m (\theta_k^{(t)} - \bar{\theta}^{(t)})(\theta_k^{(t)} - \bar{\theta}^{(t)})^\top$ , such that the inequality*

$$A^{(t)} \triangleq \eta L \left( 2T_2 + L_3^2 \Xi_t^4 + (2L_1 + 2L_3 \Xi_t^2 + \frac{mL_4^2}{24^2}) \sqrt{m} \Xi_t^3 \right) \leq 0 \quad (\text{D.10})$$

*holds. Here  $T_2 = (\nabla \mathcal{L}(\bar{\theta}^{(t)}))^\top \nabla \text{Tr}(\nabla^2 \mathcal{L}(\bar{\theta}^{(t)}) \Gamma^{(t)})$  and  $L_1, L_3, L_4$  are the upper bounds for the first, third, and fourth derivatives of  $\mathcal{L}$ , respectively.*

This condition ensures a convergence speedup of DSGD over the centralized mini-batch SGD.

**Proof Idea.** Assuming a positive lower bound  $c_t$  on the gradient norm, the term  $-T_2$  can be lower bounded by a positive term of the form  $\gamma c_t \Xi_t^2$ , where  $\gamma > 0$ . The left-hand side

$$L_3^2 \Xi_t^4 + \left(2L_1 + 2L_3 \Xi_t^2 + \frac{mL_4^2}{24^2}\right) \sqrt{m} \Xi_t^3$$

is a polynomial in  $\Xi_t$  with leading terms of order  $\Xi_t^4$  and  $\Xi_t^3$ , both exceeding the quadratic order of the right-hand side  $-2T_2 \geq 2\gamma c_t \Xi_t^2$ . As  $\Xi_t \rightarrow 0^+$ , the left side approaches zero faster than the right side remains positive, so by continuity and the intermediate value theorem there exists a sufficiently small  $\Xi_t > 0$  satisfying the inequality.

*Proof.*

**Step (A): Derivation of  $\gamma$ .** Denote  $g^{(t)} = \nabla \mathcal{L}(\bar{\theta}^{(t)})$ . Define

$$F(\delta) = \frac{\nabla^3 \mathcal{L}(\bar{\theta}^{(t)})[\delta, \delta, g^{(t)}]}{\|g^{(t)}\| \|\delta\|^2}, \quad \delta \neq 0.$$

Since  $\nabla^3 \mathcal{L}(\bar{\theta}^{(t)})[\delta, \delta, g^{(t)}] < 0$ , we have  $F(\delta) < 0$  by [Assumption 4](#). On the compact unit sphere  $S = \{\delta : \|\delta\| = 1\}$ ,  $F$  attains its maximum  $M < 0$ . We can then set  $\gamma = -M > 0$ . Then for all  $\delta$ ,

$$\nabla^3 \mathcal{L}(\bar{\theta}^{(t)})[\delta, \delta, g^{(t)}] \leq -\gamma \|g^{(t)}\| \|\delta\|^2,$$

and in particular for each  $k$ ,

$$\nabla^3 \mathcal{L}(\bar{\theta}^{(t)})[\delta_k^{(t)}, \delta_k^{(t)}, g^{(t)}] \leq -\gamma \|g^{(t)}\| \|\delta_k^{(t)}\|^2. \quad (\text{D.11})$$

The intuition behind the parameter  $\gamma$  is that it reflects the *relative degree of progressive sharpening* ([Assumption 4](#)) during training.

**Step (B): Bound on  $T_2$ .** Denote

$$\Gamma^{(t)} = \frac{1}{m} \sum_{k=1}^m \delta_k^{(t)} (\delta_k^{(t)})^\top, \quad \Xi_t^2 = \text{Tr}(\Gamma^{(t)}) = \frac{1}{m} \sum_{k=1}^m \|\delta_k^{(t)}\|^2.$$

Then

$$T_2 = (g^{(t)})^\top \nabla \text{Tr}(\nabla^2 \mathcal{L}(\bar{\theta}^{(t)}) \Gamma^{(t)}) = \frac{1}{m} \sum_{k=1}^m \nabla^3 \mathcal{L}(\bar{\theta}^{(t)})[\delta_k^{(t)}, \delta_k^{(t)}, g^{(t)}].$$

Using the bound in [Equation \(D.11\)](#),

$$T_2 \leq \frac{1}{m} \sum_{k=1}^m (-\gamma \|g^{(t)}\| \|\delta_k^{(t)}\|^2) = -\gamma \|g^{(t)}\| \Xi_t^2.$$

Therefore, we have

$$-T_2 \geq \gamma \|g^{(t)}\| \Xi_t^2 \geq \gamma c_t \Xi_t^2.$$

**Step (C): Establishing the Target Inequality.** The goal is to show that there exists  $\Xi_t^2 > 0$  with

$$L_3^2 (\Xi_t^2)^2 + \left(2L_1 + 2L_3 \Xi_t^2 + \frac{mL_4^2}{24^2}\right) \sqrt{m} (\Xi_t^2)^{3/2} \leq -2T_2.$$

Since  $-2T_2 \geq 2\gamma c_t \Xi_t^2$ , it suffices that

$$L_3^2 (\Xi_t^2)^2 + \left(2L_1 + 2L_3 \Xi_t^2 + \frac{mL_4^2}{24^2}\right) \sqrt{m} (\Xi_t^2)^{3/2} \leq 2\gamma c_t \Xi_t^2.$$

Divide by  $\Xi_t^2 > 0$ :

$$L_3^2 \Xi_t^2 + \left(2L_1 + 2L_3 \Xi_t^2 + \frac{mL_4^2}{24^2}\right) \sqrt{m} (\Xi_t^2)^{1/2} \leq 2\gamma c_t.$$

Set

$$h(u) = L_3^2 u + \left(2L_1 + 2L_3 u + \frac{mL_4^2}{24^2}\right) \sqrt{m} \sqrt{u}, \quad u > 0.$$

Then  $\lim_{u \rightarrow 0^+} h(u) = 0 < 2\gamma c_t$ . By continuity, there is  $\delta > 0$  such that for  $0 < u < \delta$ ,  $h(u) < 2\gamma c_t$ . Hence for sufficiently small  $\Xi_t^2$ , the desired inequality holds, completing the proof.  $\square$